

The Higgs sector of the $\mu\nu$ SSM and collider physics

Javier Fidalgo

*Departamento de Física Teórica UAM and Instituto de Física Teórica UAM/CSIC,
Universidad Autónoma de Madrid (UAM), Cantoblanco, 28049 Madrid, Spain
E-mail: javier.fidalgo@uam.es*

Daniel E. López-Fogliani

*Laboratoire de Physique Théorique,
Université Paris-Sud, F-91405 Orsay, France
E-mail: daniel.lopez@th.u-psud.fr*

Carlos Muñoz

*Departamento de Física Teórica UAM and Instituto de Física Teórica UAM/CSIC,
Universidad Autónoma de Madrid (UAM), Cantoblanco, 28049 Madrid, Spain
E-mail: carlos.munoz@uam.es*

Roberto Ruiz de Austri

*Instituto de Física Corpuscular UV/CSIC, Universidad de Valencia,
Edificio Institutos de Paterna, Apt. 22085, E-46071 Valencia, Spain
E-mail: rruiz@ific.uv.es*

ABSTRACT: The $\mu\nu$ SSM is a supersymmetric standard model that accounts for light neutrino masses and solves the μ problem of the MSSM by simply using right-handed neutrino superfields. Since this mechanism breaks R -parity, a peculiar structure for the mass matrices is generated. The neutral Higgses are mixed with the right- and left-handed sneutrinos producing 8×8 neutral scalar mass matrices. We analyse the Higgs sector of the $\mu\nu$ SSM in detail, with special emphasis in possible signals at colliders. After studying in general the decays of the Higgses, we focus on those processes that are genuine of the $\mu\nu$ SSM, and could serve to distinguish it from other supersymmetric models. In particular, we present viable benchmark points for LHC searches. For example, we find decays of a MSSM-like Higgs into two lightest neutralinos, with the latter decaying inside the detector leading to displaced vertices, and producing final states with 4 and 8 b -jets plus missing energy. Final states with leptons and missing energy are also found.

KEYWORDS: Supersymmetric Effective Theories, Beyond Standard Model, Higgs Physics.

Contents

1. Introduction	1
2. The $\mu\nu$SSM	3
3. Higgs sector and decays	4
3.1 Higgs sector mixings	4
3.2 Decays	6
3.3 Couplings with the Z boson and sum rules	9
4. Signals at colliders	11
5. Gravitino and colliders	19
6. Conclusions	19
A. Neutral scalar mass matrices	23
A.1 CP-even neutral scalars	23
A.2 CP-odd neutral scalars	24
B. Higgs sector couplings	25
B.1 Coupling between three CP-even Higgses	25
B.2 Coupling between one CP-even and two CP-odd Higgses	25

1. Introduction

The μ from ν Supersymmetric Standard Model ($\mu\nu$ SSM) [1, 2, 3], uses right-handed neutrino superfield(s) to generate light neutrino masses and to solve the μ -problem [4] of the Minimal Supersymmetric Standard Model (MSSM) [5]. Thus the $\mu\nu$ SSM is a minimal model in the sense that no extra singlet superfield has to be added to the spectrum for solving the μ problem, as it is e.g. the case of the Next-to-MSSM (NMSSM) [6]. The spectrum and the vacua of the $\mu\nu$ SSM were studied in [7, 8].

The superpotential of the $\mu\nu$ SSM contains, in addition to the usual Yukawas for quarks and charged leptons, Yukawas for neutrinos $Y_\nu \hat{H}_u \hat{L} \hat{\nu}^c$, terms of the type $\lambda \hat{\nu}^c \hat{H}_d \hat{H}_u$ producing an effective μ term through electroweak (EW)-scale right-handed sneutrino vacuum expectation values (VEVs), and also terms of the type $\kappa \hat{\nu}^c \hat{\nu}^c \hat{\nu}^c$ avoiding the existence of a Goldstone boson and generating EW-scale effective Majorana masses for neutrinos, i.e. giving rise to an EW-scale seesaw. Notice that, since only dimensionless trilinear couplings

are present in the superpotential of the model, the EW scale arises through the soft supersymmetry (SUSY)-breaking terms in the scalar potential. Thus all known particle physics phenomenology can be reproduced in the $\mu\nu$ SSM with only one scale. For example, *ad hoc* high-energy scales in order to generate a GUT-scale seesaw are not needed. With the EW-scale seesaw of this model, neutrino Yukawa couplings Y_ν of the order of 10^{-6} (like the electron Yukawa coupling) are sufficient to reproduce the correct neutrino masses. The neutrino sector was studied in detail in [7, 8, 9, 10], obtaining that current neutrino data (the measured mass differences and mixing angles) can be easily reproduced.

The above terms in the superpotential produce the explicit breaking of R -parity in this model. The size of the breaking can be easily understood realizing that in the limit where Y_ν are vanishing, the $\hat{\nu}^c$ are ordinary singlet superfields like the \hat{S} of the NMSSM, without any connection with neutrinos, and R -parity is therefore conserved. Once Y_ν are switched on, the $\hat{\nu}^c$ become right-handed neutrinos, and, as a consequence, R -parity is broken. Thus the breaking is small because the EW-scale seesaw implies small values for Y_ν .

Concerning cosmological issues, dark matter and baryon asymmetry have been analysed in the model. Since the lightest supersymmetric particle (LSP) is not stable when R -parity is broken, the neutralino [11] or the right-handed sneutrino [12], with very short lifetimes, are no longer candidates for the dark matter of the Universe. Nevertheless, the gravitino, present in the local SUSY version of the model, could be a good dark matter candidate as discussed in [13], where its possible detection through the observation of a monochromatic gamma-ray line in the Fermi satellite was also studied. In [14], the generation of the baryon asymmetry of the universe was analysed in detail in the context of the $\mu\nu$ SSM, with the interesting result that electroweak baryogenesis can be realized.

Summarizing, the $\mu\nu$ SSM is a very well motivated and attractive model, and, as a consequence, a complete study of possible signals at colliders is required. In this respect, there are two main features that could help to distinguish the $\mu\nu$ SSM from other SUSY models. On the one hand, since the LSP is no longer stable due to the breaking of R -parity, not all SUSY chains must yield missing energy events. In [9, 15, 16] the decays of the lightest neutralino were discussed, as well as the correlations of the decay branching ratios with the neutrino mixing angles. On the other hand, the breaking of R -parity also generates a peculiar structure for the mass matrices. In particular, the presence of right and left-handed sneutrino VEVs leads to mixing of the neutral Higgses with the sneutrinos producing 8×8 neutral scalar mass matrices. This extended Higgs sector could be very helpful for testing the $\mu\nu$ SSM.

In this work we will continue the analysis of the Higgs sector of the model started in [7], putting special emphasis in possible signals at colliders [15, 17]. In Section 2 we will briefly review the $\mu\nu$ SSM, describing the superpotential and deriving the neutral scalar potential. In Section 3 we will analyze the Higgs sector. In particular, we will study first the Higgs mixings, and second the possible Higgs decays taking place once a Higgs particle is produced at colliders. Finally, we will discuss the LEP constraints. For that we will compute the couplings of the Higgses with the Z boson, and the sum rules. In Section 4 we will concentrate on Higgs decays that are genuine of this model, and could therefore serve to distinguish it from other SUSY models in certain regions of the parameter

space. We will present a sample of numerical examples of viable benchmark points for LHC searches. For that, we will focus first our attention on the decays of a MSSM-like Higgs with a sizeable branching ratio into two lightest neutralinos. These neutralinos could decay inside the detector leading to displaced vertices. This fact could be used to distinguish the $\mu\nu$ SSM from R-parity conserving models. Also, the product of the decays can be used to distinguish it from other R-parity breaking models. Higgs-to-Higgs cascade decays will also be studied, and we will discuss an interesting benchmark point with similar signals to the NMSSM that could also serve to distinguish the $\mu\nu$ SSM from other R-parity breaking models. For completeness, we will discuss in Section 5 the possibility that gravitino dark matter in this model might alter the collider phenomenology through the decay channel neutralino to gravitino-photon. We will see that this branching ratio turns out to be negligible. Finally, the conclusions are left for Section 6.

2. The $\mu\nu$ SSM

The superpotential of the $\mu\nu$ SSM is given by [1]¹:

$$W = \epsilon_{ab} \left(Y_{u_{ij}} \hat{H}_u^b \hat{Q}_i^a \hat{u}_j^c + Y_{d_{ij}} \hat{H}_d^a \hat{Q}_i^b \hat{d}_j^c + Y_{e_{ij}} \hat{H}_d^a \hat{L}_i^b \hat{e}_j^c + Y_{\nu_{ij}} \hat{H}_u^b \hat{L}_i^a \hat{\nu}_j^c \right) - \epsilon_{ab} \lambda_i \hat{\nu}_i^c \hat{H}_d^a \hat{H}_u^b + \frac{1}{3} \kappa_{ijk} \hat{\nu}_i^c \hat{\nu}_j^c \hat{\nu}_k^c, \quad (2.1)$$

where we take $\hat{H}_d^T = (\hat{H}_d^0, \hat{H}_d^-)$, $\hat{H}_u^T = (\hat{H}_u^+, \hat{H}_u^0)$, $\hat{Q}_i^T = (\hat{u}_i, \hat{d}_i)$, $\hat{L}_i^T = (\hat{\nu}_i, \hat{e}_i)$, $i, j, k = 1, 2, 3$ are family indices, $a, b = 1, 2$ are $SU(2)_L$ indices with $\epsilon_{12} = 1$, and Y, λ, κ are dimensionless matrices, a vector, and a totally symmetric tensor, respectively. In the following the summation convention on repeated indices is implied.

Working in the framework of supergravity, the Lagrangian $\mathcal{L}_{\text{soft}}$ is given by:

$$\begin{aligned} -\mathcal{L}_{\text{soft}} = & m_{\tilde{Q}_{ij}}^2 \tilde{Q}_i^{a*} \tilde{Q}_j^a + m_{\tilde{u}_{ij}^c}^2 \tilde{u}_i^{c*} \tilde{u}_j^c + m_{\tilde{d}_{ij}^c}^2 \tilde{d}_i^{c*} \tilde{d}_j^c + m_{\tilde{L}_{ij}}^2 \tilde{L}_i^{a*} \tilde{L}_j^a + m_{\tilde{e}_{ij}^c}^2 \tilde{e}_i^{c*} \tilde{e}_j^c \\ & + m_{H_d}^2 H_d^{a*} H_d^a + m_{H_u}^2 H_u^{a*} H_u^a + m_{\tilde{\nu}_i^c}^2 \tilde{\nu}_i^{c*} \tilde{\nu}_j^c \\ & + \epsilon_{ab} \left[(A_u Y_u)_{ij} H_u^b \tilde{Q}_i^a \tilde{u}_j^c + (A_d Y_d)_{ij} H_d^a \tilde{Q}_i^b \tilde{d}_j^c + (A_e Y_e)_{ij} H_d^a \tilde{L}_i^b \tilde{e}_j^c \right. \\ & \left. + (A_\nu Y_\nu)_{ij} H_u^b \tilde{L}_i^a \tilde{\nu}_j^c + \text{c.c.} \right] \\ & + \left[-\epsilon_{ab} (A_\lambda \lambda)_i \tilde{\nu}_i^c H_d^a H_u^b + \frac{1}{3} (A_\kappa \kappa)_{ijk} \tilde{\nu}_i^c \tilde{\nu}_j^c \tilde{\nu}_k^c + \text{c.c.} \right] \\ & - \frac{1}{2} \left(M_3 \tilde{\lambda}_3 \tilde{\lambda}_3 + M_2 \tilde{\lambda}_2 \tilde{\lambda}_2 + M_1 \tilde{\lambda}_1 \tilde{\lambda}_1 + \text{c.c.} \right). \end{aligned} \quad (2.2)$$

In addition to terms from $\mathcal{L}_{\text{soft}}$, the tree-level neutral scalar potential receives the usual D and F term contributions and is given by [1, 7]:

$$V^0 = V_{\text{soft}} + V_D + V_F, \quad (2.3)$$

¹Although we assume three families of right-handed neutrinos motivated by the Standard Model generation replication pattern, a different number of right-handed neutrinos can be used.

where

$$V_{\text{soft}} = m_{H_d}^2 H_d^0 H_d^{0*} + m_{H_u}^2 H_u^0 H_u^{0*} + m_{\tilde{L}_{ij}}^2 \tilde{\nu}_i \tilde{\nu}_j^* + m_{\tilde{\nu}_{ij}^c}^2 \tilde{\nu}_i^c \tilde{\nu}_j^{c*} \\ + \left(a_{\nu_{ij}} H_u^0 \tilde{\nu}_i \tilde{\nu}_j^c - a_{\lambda_i} \tilde{\nu}_i^c H_d^0 H_u^0 + \frac{1}{3} a_{\kappa_{ijk}} \tilde{\nu}_i^c \tilde{\nu}_j^c \tilde{\nu}_k^c + \text{c.c.} \right), \quad (2.4)$$

with $a_{\nu_{ij}} \equiv (A_\nu Y_\nu)_{ij}$, $a_{\lambda_i} \equiv (A_\lambda \lambda)_i$, $a_{\kappa_{ijk}} \equiv (A_\kappa \kappa)_{ijk}$,

$$V_D = \frac{G^2}{8} (\tilde{\nu}_i \tilde{\nu}_i^* + H_d^0 H_d^{0*} - H_u^0 H_u^{0*})^2, \quad (2.5)$$

with $G^2 \equiv g_1^2 + g_2^2$, and

$$V_F = \lambda_j \lambda_j^* H_d^0 H_d^{0*} H_u^0 H_u^{0*} + \lambda_i \lambda_j^* H_d^0 H_d^{0*} \tilde{\nu}_i^c \tilde{\nu}_j^{c*} + \lambda_i \lambda_j^* H_u^0 H_u^{0*} \tilde{\nu}_i^c \tilde{\nu}_j^{c*} + \kappa_{ijk} \kappa_{lm}^* \tilde{\nu}_i^c \tilde{\nu}_l^{c*} \tilde{\nu}_k^c \tilde{\nu}_m^{c*} \\ - (\kappa_{ijk} \lambda_j^* H_d^0 H_u^{0*} \tilde{\nu}_i^c \tilde{\nu}_k^c - Y_{\nu_{ij}} \kappa_{ljk}^* H_u^0 \tilde{\nu}_i \tilde{\nu}_l^{c*} \tilde{\nu}_k^{c*} + Y_{\nu_{ij}} \lambda_j^* H_d^0 H_u^{0*} H_u^0 \tilde{\nu}_i \\ + Y_{\nu_{ij}}^* \lambda_k H_d^0 \tilde{\nu}_k^c \tilde{\nu}_i^* \tilde{\nu}_j^{c*} + \text{c.c.}) \\ + Y_{\nu_{ij}} Y_{\nu_{ik}}^* H_u^0 H_u^{0*} \tilde{\nu}_j^c \tilde{\nu}_k^{c*} + Y_{\nu_{ij}} Y_{\nu_{lk}}^* \tilde{\nu}_i \tilde{\nu}_l^* \tilde{\nu}_j^c \tilde{\nu}_k^{c*} + Y_{\nu_{ji}} Y_{\nu_{ki}}^* H_u^0 H_u^{0*} \tilde{\nu}_j \tilde{\nu}_k^*. \quad (2.6)$$

Once the EW symmetry is spontaneously broken, the neutral scalars develop in general the following VEVs:

$$\langle H_d^0 \rangle = v_d, \quad \langle H_u^0 \rangle = v_u, \quad \langle \tilde{\nu}_i \rangle = \nu_i, \quad \langle \tilde{\nu}_i^c \rangle = \nu_i^c. \quad (2.7)$$

In the following we will assume for simplicity that all parameters in the potential are real, as well as the VEVs, i.e. that CP is conserved². As a consequence, the neutral CP-even scalars are not mixed with the neutral CP-odd scalars³.

Let us now discuss in the next section the neutral Higgs sector of the model and possible signals at colliders.

3. Higgs sector and decays

In this section we will analyse the mixings in the scalar (Higgs) sector of the $\mu\nu$ SSM, and we will also study the possible decay modes of Higgses once they are generated at colliders. We will focus our attention on the novelties that this extended Higgs sector introduces compared to Higgs sectors of other models, like e.g. the one of the NMSSM. Finally, we will discuss the LEP constraints in the context of this model.

3.1 Higgs sector mixings

The presence of right and left-handed sneutrino VEVs in the $\mu\nu$ SSM leads to mixing of the neutral components of the Higgs doublets with the sneutrinos producing the 8×8 neutral

²For an analysis of spontaneous CP violation, see [8].

³In general, all neutral scalars are mixed, and since all of them get VEVs, we will call them Higgses throughout this work. To be more precise, we will use the term ‘Higgses’ for the mass eigenstates, and ‘Higgs doublets’ for $H_d^T = (H_d^0, H_d^-)$, $H_u^T = (H_u^+, H_u^0)$.

scalar mass matrices for the CP-even and CP-odd states [7] that can be found in Appendix A, where we have defined as usual

$$\begin{aligned} H_u^0 &= \frac{h_u + iP_u}{\sqrt{2}} + v_u, \quad H_d^0 = \frac{h_d + iP_d}{\sqrt{2}} + v_d, \\ \tilde{\nu}_i^c &= \frac{(\tilde{\nu}_i^c)^R + i(\tilde{\nu}_i^c)^I}{\sqrt{2}} + \nu_i^c, \quad \tilde{\nu}_i = \frac{(\tilde{\nu}_i)^R + i(\tilde{\nu}_i)^I}{\sqrt{2}} + \nu_i. \end{aligned} \quad (3.1)$$

Note that after rotating away the CP-odd would be Goldstone boson, we are left with seven states. It is also worth noticing here that in the CP-even sector the 5×5 Higgs doublets–right handed sneutrino submatrix is basically decoupled from the 3×3 left handed sneutrino submatrix, since the mixing occurs only through terms proportional to ν_i or $Y_{\nu_{ij}}$ in (A.7), (A.8) and (A.10). As discussed in [1], because of the contribution of the small couplings $Y_\nu \sim 10^{-6,-7}$ to the minimization conditions for the left-handed sneutrinos, their VEVs turn out to be small $\nu \sim 10^{-4,-5}$ GeV. Then, all terms containing Y_ν or ν are negligible compared to the rest of terms that are of the order of the EW scale. The same decoupling between Higgs doublets–right handed sneutrinos and left-handed sneutrinos is true for the CP-odd sector.

On the contrary, the mixing between Higgs doublets and right-handed sneutrinos is not necessarily small. In the CP-even sector this is given by (A.5) and (A.6):

$$M_{h_d(\tilde{\nu}_i^c)^R}^2 = -a_{\lambda_i} v_u + 2\lambda_i \lambda_j v_d \nu_j^c - 2\lambda_k \kappa_{ijk} v_u \nu_j^c - Y_{\nu_{ji}} \lambda_k \nu_j \nu_k^c - Y_{\nu_{jk}} \lambda_i \nu_j \nu_k^c, \quad (3.2)$$

$$M_{h_u(\tilde{\nu}_i^c)^R}^2 = -a_{\lambda_i} v_d + a_{\nu_{ji}} \nu_j + 2\lambda_i \lambda_j v_u \nu_j^c - 2\lambda_k \kappa_{ilk} v_d \nu_l^c + 2Y_{\nu_{jk}} \kappa_{ilk} \nu_j \nu_l^c + 2Y_{\nu_{jk}} Y_{\nu_{ji}} v_u \nu_k^c. \quad (3.3)$$

Neglecting terms proportional to $Y_{\nu_{ij}}$, ν_i , using $a_{\lambda_i} = (A_\lambda \lambda)_i$, and defining $\mu \equiv \lambda_j \nu_j^c$, one can write the above equations as

$$M_{h_d(\tilde{\nu}_i^c)^R}^2 \approx 2\lambda_i \mu v_d - 2\lambda_k \kappa_{ijk} v_u \nu_j^c - v_u (A_\lambda \lambda)_i, \quad (3.4)$$

$$M_{h_u(\tilde{\nu}_i^c)^R}^2 \approx 2\lambda_i \mu v_u - 2\lambda_k \kappa_{ilk} v_d \nu_l^c - v_d (A_\lambda \lambda)_i. \quad (3.5)$$

Let us now discuss how to suppress these mixings. This can be used to have very light $\tilde{\nu}^c$ -like Higgses avoiding collider constraints, but also, as we will discuss below, to have a doublet-like Higgs as the lightest one being as heavy as possible. The simplest possibility to suppress the mixings is that Eqs. (3.4) and (3.5) vanish. Clearly, this can be obtained with $\lambda_i \rightarrow 0$. Another possibility is that the sum of the three terms in the above equations vanishes. To simplify this analysis let us start with only one generation of right-handed neutrinos. Then,

$$0 \approx 2\lambda \mu v_u - 2\lambda \kappa v_d \nu^c - v_d A_\lambda \lambda, \quad (3.6)$$

$$0 \approx 2\lambda \mu v_d - 2\lambda \kappa v_u \nu^c - v_u A_\lambda \lambda, \quad (3.7)$$

and after a rotation in the mass matrix we obtain the condition [7]

$$A_\lambda = \frac{2\mu}{\sin 2\beta} - 2\kappa \nu^c, \quad (3.8)$$

similar to the one of the NMSSM (with $\nu^c \rightarrow S$) [18]. Following the same arguments as above, in the CP-odd sector, and after a rotation in the mass-squared matrix to isolate the Goldstone boson, we obtain the condition,

$$\lambda(A_\lambda - 2\kappa\nu^c)v = 0, \quad (3.9)$$

implying $\lambda \rightarrow 0$ or $A_\lambda = 2\kappa\nu^c$. The generalization of these results to three generations of right-handed neutrinos is straightforward. In addition to the solution $\lambda_i \rightarrow 0$, we obtain

$$A_{\lambda_i} = \frac{2\mu}{\sin 2\beta} - \frac{2}{\lambda_i} \sum_{j,k} \kappa_{ijk} \lambda_j \nu_k^c, \quad (3.10)$$

$$A_{\lambda_i} = \frac{2}{\lambda_i} \sum_{j,k} \kappa_{ijk} \lambda_j \nu_k^c, \quad (3.11)$$

for the CP-even and CP-odd sectors, respectively.

Nevertheless, although the above solutions for the decoupling of Higgs doublets and right-handed sneutrinos can be used in general, they are sufficient but not necessary conditions. As was shown in [7], there are regions of the parameter space where the off-diagonal mixing terms of the neutral scalar mass matrices are smaller than the diagonal terms, and then quite pure singlets can also be obtained. Actually, we will use this mechanism in Section 4 in order to search for interesting signals at colliders.

Let us finally emphasize that some of these conditions can be applied not only to obtain a very light $\tilde{\nu}^c$ -like lightest Higgs, as discussed above, but also to have the lightest scalar as heavy as possible⁴. Clearly this lightest scalar, for being as heavy as possible, must be Higgs doublet-like, since the right- and left-handed sneutrinos can be as heavy as we want. Thus to have it as heavy as possible the contamination with right-handed sneutrinos should be small. For this to happen the right-handed sneutrinos must be very heavy and/or the mixing should be small. Notice however that for the latter we cannot use one of the conditions discussed above, $\lambda_i \rightarrow 0$, since λ_i must be as large as possible to saturate the upper bound on the lightest Higgs boson mass [7].

3.2 Decays

Here we will study possible decay modes of the Higgses in the $\mu\nu$ SSM, pointing out novel features with respect to the NMSSM/MSSM. The presence of new fields extending the Higgs sector, and the fact that R -parity is not a symmetry of the model, give rise to new decays, thus changing substantially the phenomenology.

First of all, the Higgs-to-Higgs cascade decays can be more complicated since more Higgses are present in this model compared to the NMSSM. As discussed above, in the $\mu\nu$ SSM there are eight CP-even and seven CP-odd Higgses, while in the NMSSM there are three CP-even and two CP-odd Higgses. The relevant couplings for Higgs-to-Higgs decays in the $\mu\nu$ SSM are written in Appendix B, and the Feynman diagrams of all possible tree-level decays of the Higgses are given in Figs. 1-4. In particular, for a CP-even (CP-odd)

⁴Notice that the upper bound on the lightest Higgs boson mass for the $\mu\nu$ SSM turns out to be similar to the one of the NMSSM [7].

decaying scalar we can see in Fig. 2 that the Feynman diagrams **a** and **c** (**b**) are crucial to understand new decays with respect to the NMSSM ones. Note that the Feynman diagram(s) **b** (**a** and **c**) in the figure is (are) present only if a source of CP violation is taken into account⁵.

Let us assume that we have enough energy to generate only one CP-even Higgs at a collider, i.e., only one Higgs, h_1 , has mass below the threshold energy. Then the following decay is possible:

$$h_1 \rightarrow 2 \text{ Standard Model fermions} . \quad (3.12)$$

In case that the second lightest Higgs, h_2 , can be generated, the following cascade decay is possible if kinematically allowed:

$$h_2 \rightarrow 2h_1 \rightarrow 4 \text{ Standard Model fermions} . \quad (3.13)$$

If the third lightest Higgs, h_3 , can be generated, then if kinematically allowed we have the possibility

$$h_3 \rightarrow 2h_2 \rightarrow 4h_1 \rightarrow 8 \text{ Standard Model fermions} . \quad (3.14)$$

The situation turns out to be more complicated if we take into account the decays to scalars that are not the ones immediately below in mass. Also we have the possibility of having light pseudoscalars entering in the game. In the $\mu\nu$ SSM we have three/two (six/five including left-handed sneutrinos) pseudoscalars more than in the MSSM/NMSSM case, and they could be very light. Thus we may need to include the following decays (if kinematically allowed) into the cascades:

$$h_\alpha \rightarrow h_\beta h_\gamma , \quad h_\alpha \rightarrow P_{\beta'} P_{\gamma'} , \quad P_{\alpha'} \rightarrow P_{\beta'} h_\gamma , \quad (3.15)$$

where $\alpha, \beta, \gamma = 1, \dots, 8$ and $\alpha', \beta', \gamma' = 1, \dots, 7$.

In benchmark point 7 of Section 4 we will study an example where these types of Higgs-to-Higgs cascade decays are present. Working with a MSSM-like CP even Higgs, h_{MSSM} , it will decay into $b\bar{b}$ or through the cascades typical of the NMSSM, $h_{\text{MSSM}} \rightarrow 2P \rightarrow 2b2\bar{b}$, in most of the cases. Nevertheless we will see that the following cascade is also possible: $h_{\text{MSSM}} \rightarrow 2h \rightarrow 4P \rightarrow 4b4\bar{b}$. In benchmark point 8 we will see that h_{MSSM} can decay with the following relevant cascades: $h_{\text{MSSM}} \rightarrow 2h_1 \rightarrow 4P_{1,2} \rightarrow 4\tau^+4\tau^-$, $h_{\text{MSSM}} \rightarrow 2P_3 \rightarrow 2b2\bar{b}$, because for the singlet-like pseudoscalars $P_{1,2}$ the decay into $b\bar{b}$ is kinematically forbidden, whereas for P_3 it is allowed. These cascades are genuine of the $\mu\nu$ SSM.

Another difference of the $\mu\nu$ SSM compared to the NMSSM, that comes from the breaking of R -parity, is that a very light lightest Higgs with the decays into $b\bar{b}$ or $\tau^+\tau^-$ kinematically forbidden, could decay into two neutrinos $\nu_i\nu_j$ at the tree-level. This possibility is included in the Feynman diagram **c** of Fig. 1, due to the mixing of the MSSM

⁵In order to reduce the number of Feynman diagrams shown in the figure, we allow an abuse of notation in the diagrams, since if CP is violated, CP-even and CP-odd Higgses mix together and the notation ceases to make sense.

neutralinos and neutrinos. This decay takes place due to the presence of the superpotential terms $Y_\nu \hat{H}_u \hat{L} \hat{\nu}^c$. A Higgs with H_u composition can decay in this way because the light neutrinos, that are mainly left-handed, have small right-handed neutrino ν^c components. A Higgs with $\tilde{\nu}$ component can decay to two neutrinos because the light neutrinos can have respectively \tilde{H}_u and ν^c components. Of special interest is the fact that a Higgs with $\tilde{\nu}^c$ composition can also decay into $\nu_i \nu_j$ because the light neutrinos can have \tilde{H}_u component, as mentioned above, or through the $\kappa \hat{\nu}_i^c \hat{\nu}_j^c \hat{\nu}_k^c$ terms in the superpotential, taking into account that left- and right-handed neutrinos mix together. However, since the neutrino Yukawa couplings are small, it is difficult to compete with the usual 1-loop decay into photons through the chargino loop process (see Fig. 5). Then, the usual constraints for very light Higgses annihilating to photons [19] still apply.

Also we must take into account that, unless they are not kinematically allowed, new decays to leptons are present, as can be deduced from the Feynman diagram **d** of Fig. 1, since the charged leptons are mixed with the MSSM charginos. Then, a singlet-like Higgs could decay to charged leptons through the $\lambda \hat{\nu}^c \hat{H}_u \hat{H}_d$ terms in the superpotential, due to the chargino composition. The mixing of charged leptons with charginos also affects the loop diagrams describing Higgs decaying into photons (Fig. 5) due to the contribution from charged leptons running in the loop, since the charginos are contaminated with them. Besides, a Higgs with $\tilde{\nu}$ component can also decay into charged leptons through the $Y_e \hat{H}_d \hat{L} \hat{e}^c$ term in the superpotential. Notice that it can also decay into two light neutrinos through the contamination with \tilde{H}_u^0 and ν^c in the Yukawa term $Y_\nu \hat{H}_u \hat{L} \hat{\nu}^c$. For example, for the benchmark point 2 shown in Table 2 of Section 4, the light singlet-like pseudoscalars $P_{1,2,3}$ decay mainly into $\tau^+ \tau^-$ because of the small contamination with doublets.

An interesting situation that we will study in detail in Section 4, occurs when a MSSM-like CP even Higgs, h_{MSSM} , has a sizeable branching ratio to two light neutralinos $h_{\text{MSSM}} \rightarrow \tilde{\chi}^0 \tilde{\chi}^0$. Since R -parity is broken, neutralinos can decay into a Higgs and a neutrino inside the detector leading to displaced vertices. This possibility is included in the Feynman diagram **c** of Fig. 1, due to the mixing of the MSSM neutralinos and neutrinos. Thus working with light on-shell singlet-like pseudoscalars, cascades of the type $h_{\text{MSSM}} \rightarrow \tilde{\chi}^0 \tilde{\chi}^0 \rightarrow 2P2\nu \rightarrow 2b2\bar{b}2\nu$, leading to the final state 4 b -jets plus missing energy, will be present. If the decay of the pseudoscalars into two b 's is kinematically forbidden, then they decay into $\tau^+ \tau^-$ generating the following cascade: $h_{\text{MSSM}} \rightarrow \tilde{\chi}^0 \tilde{\chi}^0 \rightarrow 2P2\nu \rightarrow 2\tau^+ 2\tau^- 2\nu$. We will also see that the final state 8 b -jets plus missing energy is possible in situations where singlet-like scalars are produced by the decay of the neutralino, and they decay to pseudoscalars as shown in (3.15), $h_{\text{MSSM}} \rightarrow \tilde{\chi}^0 \tilde{\chi}^0 \rightarrow 2h2\nu \rightarrow 4P2\nu \rightarrow 4b4\bar{b}2\nu$. As mentioned above, in benchmark point 8 of Section 4, for the singlet-like pseudoscalars $P_{1,2}$ the decay into $b\bar{b}$ is kinematically forbidden, whereas for P_3 it is allowed, thus the following relevant cascades can be produced: $h_4 \rightarrow \tilde{\chi}_4^0 \tilde{\chi}_4^0 \rightarrow 2P_{1,2}2\nu \rightarrow 2\tau^+ 2\tau^- 2\nu$, $h_4 \rightarrow \tilde{\chi}_4^0 \tilde{\chi}_4^0 \rightarrow 2h_{1,2,3}2\nu \rightarrow 4P_{1,2}2\nu \rightarrow 4\tau^+ 4\tau^- 2\nu$, $h_4 \rightarrow \tilde{\chi}_4^0 \tilde{\chi}_4^0 \rightarrow 2P_32\nu \rightarrow 2b2\bar{b}2\nu$.

Displaced vertices are common signals of R -parity violating models and could help to distinguish the $\mu\nu\text{SSM}$ from the NMSSM. In addition, other R -parity breaking models such as the BRpV [20] do not have singlets in the spectrum, and, as a consequence, the

above decays can be considered as genuine of the $\mu\nu$ SSM. Note e.g. that in the BRpV, if the lightest neutralino is lighter than the gauge bosons, only three-body processes are available for its decay.

Regarding the charged Higgses, as was discussed in [7], they are mixed with the sleptons opening the following possibility. As usual, a slepton can decay into a neutralino and a lepton as shown in Fig. 6a. In a R -parity conserving model, if the neutralino is heavier than the slepton the latter will be stable. However, when R -parity is broken, the left-handed neutrinos mix with the neutralinos, and then the slepton decays into a lepton and a light neutrino. Since the charged Higgses are mixed with the sleptons, they can also decay in this way.

It is worth noticing here that, similarly to a slepton, a squark can decay into a quark and a light neutrino. This can be deduced from Figs. 6b and 6c using again that neutrinos and neutralinos mix together. Let us also mention that, as usual in R -parity breaking models, the squarks or the sleptons can be the LSP⁶ without conflict with experimental bounds. Whereas in the MSSM/NMSSM this would imply a stable charged particle incompatible with these bounds, in the $\mu\nu$ SSM the LSP decays.

In the next subsection we will study the couplings of the Higgses with the Z boson and the sum rules in the $\mu\nu$ SSM, discussing also the LEP constraints.

3.3 Couplings with the Z boson and sum rules

In the following we will discuss the LEP constraints, especially the ones coming from the Higgs-strahlung process shown in Fig. 7. In the previous subsection we have discussed Higgs-to-Higgs decays in the $\mu\nu$ SSM (see Eq.(3.15)). Thus a CP-even Higgs originated through a Higgs-strahlung could decay in that way.

Let us remember that LEP data can be used to set lower bounds on the lightest Higgs boson mass in non-standard models, as shown in Fig. 8 from [21]. In the ratio $\xi^2 = (g_{hZZ}/g_{hZZ}^{SM})^2$, g_{hZZ} designates the non-standard hZZ coupling and g_{hZZ}^{SM} the same coupling in the Standard Model. Whereas in Fig. 8, the Higgs boson is assumed to decay into fermions and bosons according to the Standard Model, when $BR(h \rightarrow b\bar{b})$ differs from the Standard Model one, the parameter in Fig. 8, ξ^2 , must be replaced by $\xi^2 BR(h \rightarrow b\bar{b})/BR_{SM}(h \rightarrow b\bar{b})$.

For the $\mu\nu$ SSM for each Higgs we can define the couplings ξ_α , with $\alpha = 1, \dots, 8$, given by

$$\xi_\alpha = [v_u S(u, \alpha) + v_d S(d, \alpha) + \nu_i S(L_i, \alpha)]/v, \quad (3.16)$$

where $S(u, \alpha)$, $S(d, \alpha)$, $S(L_i, \alpha)$ are the fraction composition of up-type Higgs doublet, down-type Higgs doublet and left-handed sneutrinos of the h_α neutral scalar mass eigenstate. A sum over $i = 1, 2, 3$ is assumed in the last term, and $v^2 = v_u^2 + v_d^2 + \nu_i \nu_i$.

⁶In the following we will define the LSP as the lightest supersymmetric particle present in Lagrangian when the neutrino Yukawas are set to zero. As usual in R -parity breaking models, the LSP is not really well defined. For example, the lightest scalar with a singlet sneutrino composition can be lighter than the lightest neutralino. Also the left-handed neutrinos are very light and are mixed with the MSSM neutralinos.

If more than one Higgs with mass below 114 GeV are present but they are degenerated, we could define $\xi^2 = \xi_\alpha \xi_\alpha$, where the sum is over all Higgses below 114 GeV, and still use Fig. 8 for $\xi^2 BR(h \rightarrow b\bar{b})/BR_{\text{SM}}(h \rightarrow b\bar{b})$.

Also with more than one Higgs below 114 GeV with arbitrary masses, for each Higgs these constraints can be used for the coupling $\xi_\alpha^2 BR(h_\alpha \rightarrow b\bar{b})/BR_{\text{SM}}(h \rightarrow b\bar{b})$. Notice however that, given a value of $\xi_\alpha^2 BR(h_\alpha \rightarrow b\bar{b})/BR_{\text{SM}}(h \rightarrow b\bar{b})$, the corresponding lower bound on the Higgs mass is a necessary but not sufficient condition to fulfil the LEP bounds.

Obviously, if the Higgs is mostly $\tilde{\nu}^c$ -like the coupling goes to zero, and we could have three very light Higgses avoiding the LEP constraints. From the above discussion we can see that another way to avoid them would be to make $BR(h \rightarrow b\bar{b})$ small.

However, in the general case a more involved analysis is necessary, since for example more than $2b$ in the final state are possible. Let us remember that searches for $h \rightarrow \Phi\Phi$ and $\Phi \rightarrow b\bar{b}$ (where Φ is a CP-odd or CP-even Higgs) by OPAL [22] and DELPHI [23] impose a strong constraint on the parameter space of the Standard Model. Once combined these analyses, one obtains $M_H > 110$ GeV for $\xi \sim 1$. Nevertheless, in models with more scalars and pseudoscalars it is possible to obtain a larger number of $b\bar{b}$, e.g. $h_3 \rightarrow 2h_2 \rightarrow 4P_1 \rightarrow 4b4\bar{b}$. It seems therefore that a re-analysis of the LEP data, to take into account this well motivated and complex phenomenology, would be interesting. Specially interesting would be to re-analyse the well-known 2.3σ excess in the $e^+e^- \rightarrow Z + b\bar{b}$ channel in the LEP data around 100 GeV. In the context of the NMSSM, the consistency of the excess with $h \rightarrow PP$ decays was discussed in [24].

Searches for $e^+e^- \rightarrow hZ$ independent of the decay mode of the Higgs by OPAL [25], could also be important to exclude some regions of the parameter space.

Searches for $h \rightarrow \Phi\Phi$ and $\Phi \rightarrow gg$, $\Phi \rightarrow c\bar{c}$, $\Phi \rightarrow \tau^+\tau^-$ by OPAL [26], and the recent analysis of the Higgs decaying into four taus carried out in [27], must also be taken into account. Nevertheless, the $\mu\nu$ SSM requires a more detailed analysis than the one available in the literature, since for instance a larger number of τ 's in the final states is possible.

It is also worth mentioning that an on-shell or off-shell Z could decay into neutralinos, with the three lightest neutralinos being very light and mainly composed by left-handed neutrinos. The decay of the neutralinos $\tilde{\chi}_a^0$ with $a = 4, \dots, 10$ was discussed in [9, 15]. Invisible Z width constraints [28] must be applied.

Let us finally discuss the sum rules. For the ξ_α defined in Eq. (3.16), one can obtain the following sum rule:

$$\sum_{\alpha=1}^8 \xi_\alpha^2 = 1 . \quad (3.17)$$

Notice that for the three $\tilde{\nu}$ -like Higgses the corresponding ξ_α can be neglected, and therefore one can write

$$\sum_{\phi=1}^5 \xi_\phi^2 \approx 1 , \quad (3.18)$$

where

$$\xi_\phi \approx [\sin \beta S(u, \phi) + \cos \beta S(d, \phi)] , \quad (3.19)$$

with $\tan \beta = \frac{v_u}{v_d}$ defined as usual, since the ν_i are very small as discussed above.

Also another important sum rule, in analogy with the one discussed in [29], is valid:

$$\sum_{\alpha=1}^8 \xi_\alpha^2 M_{h_\alpha}^2 = M_{\max}^2 , \quad (3.20)$$

where, neglecting terms with Y_ν and ν , M_{\max} is the upper bound on the lightest Higgs mass studied in [7]

$$M_{\max}^2 = M_Z^2 \left(\cos^2 2\beta + \frac{2\lambda_i \lambda_i \cos^2 \theta_W}{g_2^2} \sin^2 2\beta \right) + \text{rad. corr.} \quad (3.21)$$

Using Eqs. (3.17) and (3.20) one can deduce, as in the case of the NMSSM [30], that

$$M_{h_2}^2 \leq \frac{1}{1 - \xi_1^2} (M_{\max}^2 - \xi_1^2 M_{h_1}^2) , \quad (3.22)$$

where h_1 and h_2 are the lightest and next-to-lightest Higgses.

Finally let us mention that a simple way to avoid current collider constraints is to make the new Higgses very heavy, in such a way that the constraints apply only to the first one, as we will see in benchmark point 6 presented in Section 4. Then very interesting signals could be expected from the Higgs cascade decays in experiments like LHC.

4. Signals at colliders

In the previous section we have tried to provide a general overview of the decays of the Higgses of the $\mu\nu$ SSM. In this section we will concentrate in those decays that are genuine of this model, and could therefore serve to distinguish it from other SUSY models. For that, we will focus first our attention on the decays of a MSSM-like Higgs with a mass about 114 GeV (for being detectable in the near future), and with a sizeable branching ratio into the two lightest neutralinos. These neutralinos could decay inside the detector leading to displaced vertices. This fact can be used to distinguish the $\mu\nu$ SSM from R-parity conserving models such as the NMSSM. For example, as mentioned in subsection 3.2, the lightest neutralino⁷ $\tilde{\chi}_4^0$'s can decay to an on-shell light singlet pseudoscalar (that subsequently decays to $b\bar{b}$) and a neutrino, and therefore the decay $h_{MSSM} \rightarrow \tilde{\chi}_4^0 \tilde{\chi}_4^0 \rightarrow 2P2\nu \rightarrow 2b2\bar{b}2\nu$ is genuine of the $\mu\nu$ SSM. In other R-parity breaking models such as the BRpV, there are no singlet Higgses and a lightest neutralino lighter than gauge bosons could decay only through three-body decay processes. However, we have to point out that since the final decay products could be the same in both models, they may be difficult to distinguish experimentally.

⁷In our convention, when we refer to 'neutralino', we are excluding the three light left-handed neutrinos $\tilde{\chi}_{1,2,3}^0$.

We will also discuss an example where the Higg-to-Higgs cascade decays studied in subsection 3.2 are relevant to distinguish the $\mu\nu$ SSM from other SUSY models.

Following the above strategy, in this section we will present a sample of numerical examples of viable benchmark points of interest for LHC searches. The study of the heavier doublet-like Higgs, where the cascades described in subsection 3.2 could also be relevant, is left for a future work.

Let us mention that for the computation we have used a spectrum generator for the $\mu\nu$ SSM (see [7] for a description⁸), linked with modified subroutines for the model, based on the codes NMHdecay [31] and Sphenox [32]. In particular, the modified subroutines based on the code NMHdecay are used to compute the two-body decays of all Higgses present in the $\mu\nu$ SSM. We have also built a subroutine to compute the two-body decays of neutralinos. The modified subroutines based on the code Sphenox are used to compute the three-body decays of neutralinos.

We have searched for points of the parameter space that are safe from exclusion by current collider constraints but that could be detected in the near future at LHC. Nevertheless, a full analysis of these points in the light of LEP and TEVATRON is beyond the scope of this paper and then it is not possible to totally guarantee that all of them satisfy all experimental constraints. In any case, if any of the benchmark points provided here is not completely safe from experimental constraints, it would be in the border and with small variations in the values of the parameters could be driven to the allowed experimental region.

Below we give a list with all the constraints that we are imposing on the points analyzed. Some of them have already been discussed in Subsection 3.3.

First, all points are true minima of the neutral scalar potential. We have checked that tachyons do not appear and that the couplings fulfil Landau pole constraints at the GUT scale.

We have verified that all points satisfy the following 3σ neutrino sector constraints [33],

$$\begin{aligned} 7.14 < \Delta m_{sol}^2 / 10^{-5} \text{ eV}^2 < 8.19, \quad 2.06 < \Delta m_{atm}^2 / 10^{-3} \text{ eV}^2 < 2.81 \\ 0.263 < \sin^2 \theta_{12} < 0.375, \quad \sin^2 \theta_{13} < 0.046, \quad 0.331 < \sin^2 \theta_{23} < 0.644 \end{aligned} \quad (4.1)$$

We have guaranteed that current limits on sparticle masses with R-parity conserved are satisfied, excluding points with charged Higgs/sleptons, charginos, squarks and gluinos too light [34, 35]. We are being conservative, since strictly speaking these limits apply only to R-parity conserving models.

In the neutral Higgs sector we have checked the constraints on the reduced couplings \times branching ratios in terms of the masses, for all the CP-even and CP-odd scalars, in the following channels analysed at LEP:

- 1) For $e^+e^- \rightarrow hZ$ with the following decays of h ,

⁸In this version we have included one-loop corrections to neutrino masses (in general to neutralinos). These corrections have been computed in [10].

- $h \rightarrow \text{invisible}$ [36, 37]. Here we are assuming as invisible the light neutrinos. A more elaborated analysis requires a re-analysis of LEP data, taking into account for instance that neutralinos could partially contribute to the missing energy when the decay distance is comparable to the size of the detector. We have checked that in the points where the decay length of the lightest neutralino is considerably greater than $\mathcal{O}(1 \text{ m})$, considering also the LSP as invisible, the constraint is satisfied.
 - $h \rightarrow \gamma\gamma$, from LEP Higgs working group results [19].
 - $h \rightarrow b\bar{b}$, from the LEP Higgs working group [21].
 - h to two jets, from OPAL and the LEP Higgs working group, both at LEP2 [38, 39].
 - $h \rightarrow \tau^+\tau^-$, from the LEP Higgs working group [21].
 - $h \rightarrow PP$ with PP decaying to 4 jets, 2 jets + cc, 2 jets + $\tau^+\tau^-$, 4 $\tau's$, cccc, $\tau\tau + cc$, from OPAL results [26].
- 2) For $e^+e^- \rightarrow hP$ with hP decaying into 4 b , 4 τ , and $PPP \rightarrow 6b$ studied by DELPHI [23].
- 3) For $e^+e^- \rightarrow hZ \rightarrow PPZ \rightarrow 4b + 2jets$ the DELPHI constraints [23].
- 4) For $e^+e^- \rightarrow hZ$ independent of h decay mode, combining the results of ALEPH and OPAL collaborations [36, 21].

On the other hand, as discussed in detail in [7], using the eight minimization conditions for the neutral scalar potential we have solved the soft masses m_{H_u} , m_{H_d} , $m_{\tilde{L}_i}$ and $m_{\tilde{\nu}_i^c}$ in terms of $\tan\beta$, ν_i^c , ν_i , and we have used the fact that ν_i are very small in order to define $\tan\beta \approx \frac{v_u}{v_d}$ and $v^2 \approx v_u^2 + v_d^2$, as usual. For simplicity, to perform the numerical analysis we have assumed a diagonal structure of the parameters in flavour space. We have also assumed universality for most of the parameters. In the case of the neutrino parameters this is not possible, since we need at least two generations with different Y_{ν_i} and ν_i in order to guarantee the correct hierarchy of neutrino masses. Besides, an exact universality of the other parameters would produce degenerations in the spectrum. Since we are working with low-energy parameters, the presence of exact universality after the running from higher scales seems to be extremely unlikely. To avoid this artificial situation, but still maintaining the simplicity of using universal parameters in the computation, we have slightly broken the universality in the diagonal entries of the κ tensor. On the other hand, in the case of the trilinear terms we take all of them proportional to the corresponding Yukawa couplings.

To summarize, the independent low-energy free parameters that we are varying in our analysis are,

$$\lambda_i = \lambda, \quad \tan\beta, \quad \kappa_{iii}, \quad \nu_i^c = \nu^c, \quad \nu_1, \quad \nu_2 = \nu_3, \quad Y_{\nu_1}, \quad Y_{\nu_2} = Y_{\nu_3}, \quad A_\lambda, \quad A_\kappa, \quad M_2, \quad (4.2)$$

where for M_1 and M_3 we are assuming a relation that mimics the one coming from unification at the GUT scale, $M_1 = \frac{\alpha_1^2}{\alpha_2} M_2$, $M_3 = \frac{\alpha_3^2}{\alpha_2} M_2$, implying $M_1 \approx 0.5 M_2$, $M_3 = 2.7 M_2$. In

addition we have fixed the following soft parameters as, $m_{\tilde{Q}} = 1000 \text{ GeV}$, $m_{\tilde{u}} = 1000 \text{ GeV}$, $m_{\tilde{d}} = 1000 \text{ GeV}$, $m_{\tilde{e}} = 1000 \text{ GeV}$, $A_e = 1000 \text{ GeV}$, $A_u = 2400 \text{ GeV}$, $A_d = 1000 \text{ GeV}$, $A_\nu = -1000 \text{ GeV}$. Let us remark, nevertheless, that we have varied the value of A_u for certain points, since it is relevant for the 1-loop corrections to the mass of the Standard Model Higgs.

For the values of the parameters that we will use in the benchmark points below, it is possible to show [7] using Appendix A that the mixing between the Higgses and the right-handed sneutrinos is of the order of $a_{\lambda_i} v_u = A_\lambda \lambda v_u$, and therefore small compared with the relevant diagonal terms $\lambda_i \lambda_j \nu_i^c \nu_j^c = 9\lambda^2 (\nu^c)^2$. Thus the Higgs doublets are basically decoupled from the right-handed sneutrinos. Note also that the right-handed neutrino masses are given by a value that can be approximated as $2\kappa_{iii} \nu^c$ [7].

Taking all the above into account, let us discuss now eight interesting benchmark points for collider physics. For the first three points that we will consider, the lightest neutralino $\tilde{\chi}_4^0$ is mainly a right-handed neutrino, since we take the value of $2\kappa_{iii} \nu^c$ small compared to the soft gaugino mass M_2 and Higgsino masses $\mu = \lambda_i \nu_i^c$. This composition of the LSP is genuine of the $\mu\nu$ SSM and hence, very interesting to study. The other right-handed neutrino-like neutralinos $\tilde{\chi}_{5,6}^0$ are slightly heavier than $\tilde{\chi}_4^0$, and once produced in the decay of a Higgs, they decay rapidly to $\tilde{\chi}_4^0$ through 3-body processes such as $\tilde{\chi}_{5,6}^0 \rightarrow \tilde{\chi}_4^0 q \bar{q}$ or $\tilde{\chi}_{5,6}^0 \rightarrow \tilde{\chi}_4^0 \bar{l} l$.

On the other hand, for benchmark points 4, 5 and 6, the lightest neutralino $\tilde{\chi}_4^0$ is MSSM-like. For example, taking small enough values for M_2 one can have a MSSM lightest neutralino almost bino-like. The right-handed neutrino-like neutralinos $\tilde{\chi}_{5,6,7}^0$ also decay through three-body processes to the lightest one and quarks/leptons very promptly.

Thus, additional quarks or leptons are present in the cascades due to the decays of the right-handed neutrino-like neutralinos into the lightest one.

Finally, in benchmark points 7 and 8 we work again with the lightest neutralino as a right-handed neutrino, although for benchmark point 7 it does not play an important role in the Higgs cascades and only Higgs-to-Higgs cascade decays are relevant.

Let us also remark that for all the eight benchmark points, A_κ is chosen small for having light pseudoscalars, since its contribution is the dominant one in the diagonal element of the mass matrix. In this way the neutralino can decay into a light pseudoscalar and a neutrino through two-body processes. Since we have light singlets, we are also choosing for simplicity small values of $\tan \beta$ in order to be able to fulfill LEP constraints more easily.

Benchmark point 1 is presented in Table 1. There we only show the relevant masses and branching ratios for our discussion. The masses of the heavier doublet-like Higgs and left-handed sneutrinos (both scalars or pseudoscalars) are larger than the ones shown, and we do not study the decays of such Higgses. Neither the heavier MSSM-like neutralinos $\tilde{\chi}_{7,8,9,10}^0$ play any role on our discussion. In this benchmark point a doublet-like Higgs with mass $m_{h_4} = 118.8 \text{ GeV}$ can decay into two neutralinos with masses $m_{\tilde{\chi}^0} \approx 34 - 42 \text{ GeV}$, and with a branching ratio of 4%. The lightest neutralino can decay through a two-body decay process to a scalar/pseudoscalar and a neutrino. Note that the branching ratios of the decays of neutralinos are referred only to two-body processes, while the decay lengths shown in the tables take into account two- and three-body processes. The decay into a

pseudoscalar $P_{1,2,3}$ and a neutrino takes place in 67% of the cases. These pseudoscalars are mainly decaying into $b\bar{b}$ and a displaced vertex could be detected since the decay length of the lightest neutralino is 23 cm. Besides the cascade $h_4 \rightarrow \tilde{\chi}^0 \tilde{\chi}^0 \rightarrow 2P2\nu \rightarrow 2b2\bar{b}2\nu$, the lightest neutralino could also decay to a CP-even singlet and a neutrino in 33% of the cases, with the CP-even Higgs decaying into two pseudoscalars. Then, the following cascade is also relevant: $h_4 \rightarrow \tilde{\chi}^0 \tilde{\chi}^0 \rightarrow 2h2\nu \rightarrow 4P2\nu \rightarrow 4b4\bar{b}2\nu$, leading to 8 b -jets plus missing energy with a displaced vertex.

Benchmark point 2 is given in Table 2. In this case the decay of the Standard Model Higgs with a mass $m_{h_4} = 116.2$ GeV into neutralinos is enhanced to 12%, since neutralino masses are smaller than in benchmark point 1 due to the smaller value of $2\kappa_{iii}\nu^c$. Besides, the decay of the lightest neutralino into CP-even Higgses is kinematically forbidden. Notice also that in this case the decay of the pseudoscalars into two b 's is kinematically forbidden and then they decay into $\tau^+\tau^-$. Summarizing, the following cascade leading to a displaced vertex takes place: $h_4 \rightarrow \tilde{\chi}^0 \tilde{\chi}^0 \rightarrow 2P2\nu \rightarrow 2\tau^+2\tau^-2\nu$. The decay length of the neutralino $\tilde{\chi}_4^0$ is 1.89 m.

Benchmark point 3 is given in Table 3. A doublet-like Higgs with mass $m_{h_4} = 116.6$ GeV can decay into two neutralinos with masses $m_{\tilde{\chi}^0} \approx 47 - 50$ GeV in 0.5% of the cases, with the interesting cascade $h_4 \rightarrow \tilde{\chi}^0 \tilde{\chi}^0 \rightarrow 2P2\nu \rightarrow 2b2\bar{b}2\nu$. The decay length of the lightest neutralino $\tilde{\chi}_4^0$ is 12 cm.

Let us finally remark that, as expected, we have observed that increasing the mass of the lightest neutralino, its decay length is reduced. On the other hand, reducing the mass of the light pseudoscalars a few GeV, the decay into two b 's can be kinematically forbidden, producing a dominant decay to leptons. Also it is possible to decrease the mass of the Higgs to values about 100 GeV, and then have a Higgs scenario in the line of the work [24], escaping the large fine-tuning and little hierarchy problems. We would also like to point out that, as was shown in [7], modifying the value of λ , it is possible to increase the mass of the MSSM-like Higgs up to about 140 GeV.

The input parameters of the benchmark point 4, presented in Table 4, are similar to those of the benchmark point 3, except for the fact that we are decreasing the soft gaugino mass M_2 , and therefore generating a MSSM-like lightest neutralino (almost bino-like). Thus the production through the Standard Model-like Higgs decay is increased to 42%. Notice that while in the previous benchmark points only three neutralinos $\tilde{\chi}_{4,5,6}^0$ have masses below half of the mass of the Standard Model Higgs h_4 , here four neutralinos $\tilde{\chi}_{4,5,6,7}^0$ fulfill that condition. The lightest neutralino has a decay length of 1.65 m and decays into a pseudoscalar $P_{1,2,3}$ and a neutrino, with the pseudoscalar decaying 93% of the cases into two b 's. In this case, the production of b 's described through the cascade decays of the Standard Model Higgs, leading to displaced vertices, $h_4 \rightarrow \tilde{\chi}^0 \tilde{\chi}^0 \rightarrow 2P2\nu \rightarrow 2b2\bar{b}2\nu$, is very enhanced and competes with a similar branching ratio for the direct decay of the Standard Model Higgs into two b 's.

Benchmark point 5 is given in Table 5. It is very similar to benchmark point 4, but reducing the trilinear soft term A_u , that is important for the 1-loop corrections to the mass of the Higgs, we can decrease the Standard Model Higgs mass to $m_{h_4} \sim 112.8$ GeV. LEP constraints are still satisfied since the branching ratio of h_4 into two b 's is dramatically

reduced in favour of the branching ratio to neutralinos. We have checked that in this case, the process $h_4 \rightarrow \tilde{\chi}^0 \tilde{\chi}^0 \rightarrow 2P2\nu \rightarrow 2b2\bar{b}2\nu$ satisfies the $4b$'s LEP constraint. We have also checked that the invisible Higgs constraint is satisfied even if we consider the lightest neutralino as invisible. Nevertheless, a more involved analysis of LEP data would be necessary regarding this point, to take into account the missing energy carried by the neutrinos.

Benchmark point 6 is presented in Table 6. In this case, the spectrum is heavier, with all CP-even singlet scalars above 114 GeV , and with h_1 being the Standard Model Higgs. The pseudoscalars are also considerably heavier than in the other benchmark points. This case is similar to the usual ones of the MSSM. The small difference comes from the fact that the Standard Model Higgs would decay in a significant ratio of 2% to neutralinos leading to displaced vertices. The lightest neutralino, MSSM-like, will have two-body decays kinematically forbidden and will decay only through three-body processes with a decay length of 5.33 m. In Table 6 we show the branching ratios to the following decay products (with a notation neglecting the mixings): νll , $lq\bar{q}$, $\nu q\bar{q}$, 3ν .

Benchmark point 7 is presented in Table 7. In this case, the universality assumption has been broken also for the λ_i parameters in order to favour the decay of h_4 to two singlet-like scalars h_1 . Now the neutralino does not play an important role in the cascade decays of the Higgs, since the branching ratio of h_4 into two neutralinos is very suppressed. This is due to the fact that the only kinematically-allowed decay of Higgs to neutralinos is $h_4 \rightarrow \tilde{\chi}_4^0 \tilde{\chi}_4^0$, and $\tilde{\chi}_4^0$ is a quite pure right-handed neutrino-like. As a consequence, displaced vertices are not expected for this benchmark point. The MSSM-like Higgs with a mass $m_{h_4} = 119.6 \text{ GeV}$ will have the typical decay of the MSSM into $b\bar{b}$ or the typical cascades of the NMSSM, $h_4 \rightarrow 2P \rightarrow 2b2\bar{b}$, in most of the cases. Besides, the decay of the Higgs h_4 into two CP-even singlet-like Higgses with a branching ratio of 4% is also possible. Thus the following cascade is relevant $h_4 \rightarrow 2h_1 \rightarrow 4P \rightarrow 4b4\bar{b}$. These cascades serve to distinguish the $\mu\nu$ SSM from other R-parity violating models. Besides, once a SUSY particle is produced at the collider, decaying into the LSP, the displaced vertex could allow to distinguish the $\mu\nu$ SSM from the NMSSM.

Finally, let us discuss benchmark point 8 shown in Table 8, where we work again with a right-handed neutrino-like lightest neutralino. The main feature of this case is that, whereas for the singlet-like pseudoscalars $P_{1,2}$ the decay into $b\bar{b}$ is kinematically forbidden, for P_3 it is allowed. Then, several cascade decays are expected. The MSSM-like Higgs, h_4 , has a mass of 120.2 GeV . Apart from the typical decay of the MSSM, $h_4 \rightarrow b\bar{b}$, it can also decay without leading to displaced vertices with the following relevant cascades: $h_4 \rightarrow 2h_1 \rightarrow 4P_{1,2} \rightarrow 4\tau^+4\tau^-$, $h_4 \rightarrow 2P_3 \rightarrow 2b2\bar{b}$. This signal could be considered as genuine of the $\mu\nu$ SSM. The MSSM-like Higgs can also decay into neutralinos in 6% of the cases leading to the following relevant cascades, where displaced vertices and missing energy are expected: $h_4 \rightarrow \tilde{\chi}_4^0 \tilde{\chi}_4^0 \rightarrow 2P_{1,2}2\nu \rightarrow 2\tau^+2\tau^-2\nu$, $h_4 \rightarrow \tilde{\chi}_4^0 \tilde{\chi}_4^0 \rightarrow 2h_{1,2,3}2\nu \rightarrow 4P_{1,2}2\nu \rightarrow 4\tau^+4\tau^-2\nu$, $h_4 \rightarrow \tilde{\chi}_4^0 \tilde{\chi}_4^0 \rightarrow 2P_32\nu \rightarrow 2b2\bar{b}2\nu$. This benchmark point shows how extremely characteristic signals could be expected in certain regions of the parameter space of the $\mu\nu$ SSM.

λ	κ_{111}	κ_{222}	κ_{333}	A_κ (GeV)	M_2 (GeV)
1.0×10^{-1}	2.1×10^{-2}	1.9×10^{-2}	1.7×10^{-2}	-5.0	-1.7×10^3
$\tan \beta$	A_λ (GeV)	ν_1 (GeV)	$\nu_{2,3}$ (GeV)	Y_{ν_1}	$Y_{\nu_{2,3}}$
3.9	1.0×10^3	2.61×10^{-5}	1.31×10^{-4}	5.56×10^{-8}	2.66×10^{-7}
ν^c (GeV)	m_{h_1} (GeV)	m_{h_2} (GeV)	m_{h_3} (GeV)	m_{h_4} (GeV)	m_{P_1} (GeV)
1.0×10^3	27.9	33.3	37.9	118.8	12.2
m_{P_2} (GeV)	m_{P_3} (GeV)	$m_{\tilde{\chi}_4^0}$ (GeV)	$m_{\tilde{\chi}_5^0}$ (GeV)	$m_{\tilde{\chi}_6^0}$ (GeV)	—
13.8	20.3	34.4	38.4	42.5	—
$BR(h_4 \rightarrow \sum_{i,j=4}^6 \tilde{\chi}_i^0 \tilde{\chi}_j^0)$	$BR(\tilde{\chi}_4^0 \rightarrow \sum_{i=1}^3 P_i \nu)$	$BR(\tilde{\chi}_4^0 \rightarrow h_1 \nu)$	$BR(h_1 \rightarrow \sum_{i,j=1}^3 P_i P_j)$	$BR(P_{1,2,3} \rightarrow b\bar{b})$	$l_{\tilde{\chi}_4^0 \rightarrow}^{\tau^+ \tau^-}$ (cm)
0.04	0.67	0.33	0.89	0.93	23

Table 1: Relevant input parameters, masses and branching ratios of benchmark point 1.

λ	κ_{111}	κ_{222}	κ_{333}	A_κ (GeV)	M_2 (GeV)
1.0×10^{-1}	7.7×10^{-3}	7.5×10^{-3}	7.3×10^{-3}	-1.0	-1.7×10^3
$\tan \beta$	A_λ (GeV)	ν_1 (GeV)	$\nu_{2,3}$ (GeV)	Y_{ν_1}	$Y_{\nu_{2,3}}$
3.7	1.0×10^3	2.92×10^{-5}	1.46×10^{-4}	2.70×10^{-8}	1.51×10^{-7}
ν^c (GeV)	m_{h_1} (GeV)	m_{h_2} (GeV)	m_{h_3} (GeV)	m_{h_4} (GeV)	m_{P_1} (GeV)
8.0×10^2	13.6	13.9	17.0	116.2	8.4
m_{P_2} (GeV)	m_{P_3} (GeV)	$m_{\tilde{\chi}_4^0}$ (GeV)	$m_{\tilde{\chi}_5^0}$ (GeV)	$m_{\tilde{\chi}_6^0}$ (GeV)	—
9.5	9.6	11.8	12.2	14.0	—
$BR(h_4 \rightarrow \sum_{i,j=4}^6 \tilde{\chi}_i^0 \tilde{\chi}_j^0)$	$BR(\tilde{\chi}_4^0 \rightarrow \sum_{i=1}^3 P_i \nu)$	$BR(P_1 \rightarrow \tau^+ \tau^-)$	$BR(P_2 \rightarrow \tau^+ \tau^-)$	$BR(P_3 \rightarrow \tau^+ \tau^-)$	$l_{\tilde{\chi}_4^0 \rightarrow}^{\tau^+ \tau^-}$ (cm)
0.12	1.0	0.89	0.83	0.82	189

Table 2: Relevant input parameters, masses and branching ratios of benchmark point 2.

λ	κ_{111}	κ_{222}	κ_{333}	A_κ (GeV)	M_2 (GeV)
1.0×10^{-1}	3.1×10^{-2}	3.0×10^{-2}	2.9×10^{-2}	-1.0	-1.7×10^3
$\tan \beta$	A_λ (GeV)	ν_1 (GeV)	$\nu_{2,3}$ (GeV)	Y_{ν_1}	$Y_{\nu_{2,3}}$
3.7	1.0×10^3	3.04×10^{-5}	1.18×10^{-4}	5.10×10^{-8}	2.95×10^{-7}
ν^c (GeV)	m_{h_1} (GeV)	m_{h_2} (GeV)	m_{h_3} (GeV)	m_{h_4} (GeV)	m_{P_1} (GeV)
8.0×10^2	46.0	47.9	49.5	116.6	14.6
m_{P_2} (GeV)	m_{P_3} (GeV)	$m_{\tilde{\chi}_4^0}$ (GeV)	$m_{\tilde{\chi}_5^0}$ (GeV)	$m_{\tilde{\chi}_6^0}$ (GeV)	—
14.8	16.6	46.7	48.4	50.3	—
$BR(h_4 \rightarrow \sum_{i,j=4}^6 \tilde{\chi}_i^0 \tilde{\chi}_j^0)$	$BR(\tilde{\chi}_4^0 \rightarrow \sum_{i=1}^3 P_i \nu)$	$BR(P_{1,2,3} \rightarrow b\bar{b})$	$l_{\tilde{\chi}_4^0 \rightarrow}^{\tau^+ \tau^-}$ (cm)	—	—
0.005	1.0	0.93	12	—	—

Table 3: Relevant input parameters, masses and branching ratios of benchmark point 3.

λ	κ_{111}	κ_{222}	κ_{333}	A_κ (GeV)	M_2 (GeV)
1.0×10^{-1}	3.6×10^{-2}	3.5×10^{-2}	3.4×10^{-2}	-1.0	-1.0×10^2
$\tan \beta$	A_λ (GeV)	ν_1 (GeV)	$\nu_{2,3}$ (GeV)	Y_{ν_1}	$Y_{\nu_{2,3}}$
3.7	1.0×10^3	4.11×10^{-6}	1.59×10^{-5}	4.89×10^{-8}	3.27×10^{-7}
ν^c (GeV)	m_{h_1} (GeV)	m_{h_2} (GeV)	m_{h_3} (GeV)	m_{h_4} (GeV)	m_{P_1} (GeV)
8.0×10^2	53.7	55.7	57.4	119.7	15.5
m_{P_2} (GeV)	m_{P_3} (GeV)	$m_{\tilde{\chi}_4^0}$ (GeV)	$m_{\tilde{\chi}_5^0}$ (GeV)	$m_{\tilde{\chi}_6^0}$ (GeV)	$m_{\tilde{\chi}_7^0}$ (GeV)
15.7	17.9	51.8	54.8	56.6	58.9
$BR(h_4 \rightarrow \sum_{i,j=4}^7 \tilde{\chi}_i^0 \tilde{\chi}_j^0)$	$BR(\tilde{\chi}_4^0 \rightarrow \sum_{i=1}^3 P_i \nu)$	$BR(P_{1,2,3} \rightarrow b\bar{b})$	$l_{\tilde{\chi}_4^0 \rightarrow}^{\tau^+ \tau^-}$ (cm)	—	—
0.42	1.0	0.93	165	—	—

Table 4: Relevant input parameters, masses and branching ratios of benchmark point 4.

Let us finally discuss in more detail the detectability of these signals at the LHC. For that we need to study first the production cross section of the Higgs in the context of the

λ	κ_{111}	κ_{222}	κ_{333}	A_κ (GeV)	M_2 (GeV)
1.0×10^{-1}	3.6×10^{-2}	3.5×10^{-2}	3.4×10^{-2}	-1.0	-1.0×10^2
$\tan \beta$	A_λ (GeV)	ν_1 (GeV)	$\nu_{2,3}$ (GeV)	Y_{ν_1}	$Y_{\nu_{2,3}}$
3.7	1.0×10^3	4.11×10^{-6}	1.59×10^{-5}	4.89×10^{-8}	3.27×10^{-7}
ν^c (GeV)	A_u (GeV)	m_{h_1} (GeV)	m_{h_2} (GeV)	m_{h_3} (GeV)	m_{h_4} (GeV)
8.0×10^2	1.2×10^3	53.3	55.6	57.4	112.8
m_{P_1} (GeV)	m_{P_2} (GeV)	m_{P_3} (GeV)	$m_{\tilde{\chi}_4^0}$ (GeV)	$m_{\tilde{\chi}_5^0}$ (GeV)	$m_{\tilde{\chi}_6^0}$ (GeV)
15.4	15.6	17.8	51.7	54.8	56.5
$m_{\tilde{\chi}_2^0}$ (GeV)	$BR(h_4 \rightarrow \sum_{i,j=4}^7 \tilde{\chi}_i^0 \tilde{\chi}_j^0)$	$BR(\tilde{\chi}_4^0 \rightarrow \sum_{i=1}^3 P_i \nu)$	$BR(P_{1,2,3} \rightarrow b\bar{b})$	$l_{\tilde{\chi}_4^0 \rightarrow \gamma}$ (cm)	—
58.9	0.30	1.0	0.93	164	—

Table 5: Relevant input parameters, masses and branching ratios of benchmark point 5.

$\mu\nu$ SSM. It is well known that gluon fusion and b -quark fusion are the two main production processes of a Higgs at the LHC in the context of SUSY. Gluon fusion dominates over b -quark fusion in our benchmark points, as can be shown using the relevant equations [40]:

$$\sigma(gg \rightarrow h_4) = \sigma(gg \rightarrow H_{\text{SM}}) \frac{\Gamma(h_4 \rightarrow gg)}{\Gamma(H_{\text{SM}} \rightarrow gg)} \simeq \sigma(gg \rightarrow H_{\text{SM}}) , \quad (4.3)$$

$$\sigma(b\bar{b} \rightarrow h_4) = \sigma(b\bar{b} \rightarrow H_{\text{SM}}) \left(\frac{Y_{bbh_4}}{Y_{bbH_{\text{SM}}}} \right)^2 = \sigma(b\bar{b} \rightarrow H_{\text{SM}}) \frac{S^2(d, 4)}{\cos^2 \beta} . \quad (4.4)$$

We can see that for the case of b -quark fusion, the production cross section is reduced compared to the one of the Standard Model because in our benchmark points the value of $\tan \beta$ is low, and the main component of the Higgs is H_u^0 . However, the production cross section for gluon fusion is very similar to the one of the Standard Model. Note that in all benchmark points studied, we were interested in the production of a doublet-like Higgs (h_4 in our notation, except for the benchmark point 6 where it is the lightest Higgs and therefore is denoted as h_1). In addition, our gluinos and squarks are heavy, and as a consequence the decay width into gluons is very similar to the one of the Standard Model.

We have used the code HIGLU [41] to compute explicitly the production cross section of a Standard Model Higgs and the decay widths into gluons for our benchmark points, finding that $0.75 \sigma(gg \rightarrow H_{\text{SM}}) \lesssim \sigma(gg \rightarrow h_4) \lesssim \sigma(gg \rightarrow H_{\text{SM}})$. For a center of mass energy of 7 TeV we find that $\sigma(gg \rightarrow H_{\text{SM}})$ is about 17 – 19.5 pb and, as a consequence, we obtain production cross sections of about $\sigma(gg \rightarrow h_4) \simeq 15 - 19$ pb. Then, in principle we expect that the LHC could detect the signals described in this paper except maybe for cascades with a very small branching ratio (see Table 9). For example, the cascade described above with the largest value of the product of the cross section multiplied by the branching ratio is the one of the benchmark point 4, $h_4 \rightarrow \tilde{\chi}_4^0 \tilde{\chi}_4^0 \rightarrow 2P2\nu \rightarrow 2b2\bar{b}2\nu$, with a result of 5860 fb. The cascade with the smallest value of this product is the one of the benchmark point 8, $h_4 \rightarrow \tilde{\chi}_4^0 \tilde{\chi}_4^0 \rightarrow 2P_32\nu \rightarrow 2b2\bar{b}2\nu$, with a result of 20 fb. The study of the detectability of these signals at the LHC with an event generator is beyond the scope of this paper and is left for a future work.

λ	κ_{111}	κ_{222}	κ_{333}	A_κ (GeV)	M_2 (GeV)
1.12×10^{-1}	7.12×10^{-2}	7.11×10^{-2}	7.10×10^{-2}	-18	-1.0×10^2
$\tan \beta$	A_λ (GeV)	ν_1 (GeV)	$\nu_{2,3}$ (GeV)	Y_{ν_1}	$Y_{\nu_{2,3}}$
3.7	1.0×10^3	7.21×10^{-7}	1.04×10^{-7}	6.66×10^{-8}	4.53×10^{-7}
ν^c (GeV)	m_{h_1} (GeV)	m_{h_2} (GeV)	m_{h_3} (GeV)	m_{h_4} (GeV)	m_{P_1} (GeV)
8.47×10^2	113.7	115.1	115.3	118.9	57.8
m_{P_2} (GeV)	m_{P_3} (GeV)	$m_{\tilde{\chi}_4^0}$ (GeV)	$m_{\tilde{\chi}_5^0}$ (GeV)	$m_{\tilde{\chi}_6^0}$ (GeV)	$m_{\tilde{\chi}_7^0}$ (GeV)
57.9	61.3	52.1	114.2	120.2	120.4
$BR(h_1 \rightarrow \tilde{\chi}_4^0 \tilde{\chi}_4^0)$	$BR(\tilde{\chi}_4^0 \rightarrow l q \bar{q})$	$BR(\tilde{\chi}_4^0 \rightarrow \nu l \bar{l})$	$BR(\tilde{\chi}_4^0 \rightarrow \nu q \bar{q})$	$BR(\tilde{\chi}_4^0 \rightarrow 3\nu)$	$l_{\tilde{\chi}_4^0 \rightarrow \gamma}$ (cm)
0.02	0.52	0.28	0.15	0.05	533

Table 6: Relevant input parameters, masses and branching ratios of benchmark point 6.

5. Gravitino and colliders

As was mentioned in the Introduction, since R -parity is broken in the $\mu\nu$ SSM, neutralinos or sneutrinos, with very short lifetimes, are no longer candidates for the dark matter of the Universe. Nevertheless, if the gravitino $\Psi_{3/2}$ is the LSP, it was shown in [13] that it could be a good candidate for dark matter, with a lifetime much longer than the age of the Universe. There, it was also shown that because the gravitino decays producing a monochromatic photon, the indirect detection of gravitinos in the *Fermi* satellite [42] with a mass range between 0.1-10 GeV is possible. Larger masses are disfavored by current *Fermi* measurements.

In this case of gravitino LSP, one should check whether or not the collider signals studied in the previous section, are altered. In particular, the neutralino partial decay length into gravitino and photon must be computed. For this computation we can use the expression of the decay length $\tilde{\chi}_4^0 \rightarrow \Psi_{3/2} \gamma$ [43]. One obtains:

$$c \tau_{\tilde{\chi}_4^0}^{3/2} \sim 80 \text{ km} \left(\frac{m_{3/2}}{10 \text{ keV}} \right)^2 \left(\frac{m_{\tilde{\chi}_4^0}}{50 \text{ GeV}} \right)^{-5}. \quad (5.1)$$

We can easily see that in order to have a significant decay to gravitinos, the mass of the gravitino must be very low, less than 10 keV. That is, for gravitino masses larger than 10 keV, the decay width of neutralino into gravitino and photon is much smaller than the decay widths into Standard Model particles. Thus the collider signals studied in the previous section are not altered.

Summarizing, we want to emphasize that in the $\mu\nu$ SSM the gravitino could be a viable dark matter candidate, accessible to indirect detection experiments, and without altering the collider phenomenology described along this paper.

6. Conclusions

In this work we have studied the Higgs sector of the $\mu\nu$ SSM focusing our attention on collider physics. In certain regions of the parameter space, the phenomenology of the Higgs sector in this model is very rich and different from other SUSY models. On the one

$\lambda_{1,2}$	λ_3	$\tan \beta$	A_λ (GeV)	A_κ (GeV)	M_2 (GeV)
1.0×10^{-2}	2.8×10^{-1}	3.7	1.0×10^3	-1	-5.88×10^3
κ_{111}	κ_{222}	κ_{333}	Y_{ν_1}	Y_{ν_2}	Y_{ν_3}
7.12×10^{-2}	6.95×10^{-2}	3.15×10^{-2}	8.58×10^{-8}	2.42×10^{-7}	2.13×10^{-6}
ν_1 (GeV)	ν_2 (GeV)	ν_3 (GeV)	ν^c (GeV)		—
1.19×10^{-4}	1.71×10^{-4}	4.72×10^{-7}	8.0×10^2		—
m_{h_1} (GeV)	m_{h_2} (GeV)	m_{h_3} (GeV)	m_{h_4} (GeV)	$m_{P_{1,2}}$ (GeV)	m_{P_3} (GeV)
47.9	110.9	113.6	119.6	14.0	25.7
$m_{\tilde{\chi}_4^0}$ (GeV)	$m_{\tilde{\chi}_5^0}$ (GeV)	$m_{\tilde{\chi}_{6,7}^0}$ (GeV)	—	—	—
53.9	111.2	113.9	—	—	—
$BR(h_4 \rightarrow h_1 h_1)$	$BR(h_1 \rightarrow \sum_{i,j=1}^3 P_i P_j)$	$BR(P_i \rightarrow b\bar{b})$	$BR(h_4 \rightarrow \sum_{i,j=1}^3 P_i P_j)$	$BR(h_4 \rightarrow b\bar{b})$	—
0.04	0.97	0.93	0.39	0.40	—

Table 7: Relevant input parameters, masses and branching ratios of benchmark point 7.

λ	κ_{111}	κ_{222}	κ_{333}	A_κ (GeV)	M_2 (GeV)
1.0×10^{-1}	1.66×10^{-2}	1.65×10^{-2}	1.64×10^{-2}	-5.0	-1.7×10^3
$\tan \beta$	A_λ (GeV)	ν_1 (GeV)	$\nu_{2,3}$ (GeV)	Y_{ν_1}	$Y_{\nu_{2,3}}$
4.9	1.0×10^3	5.84×10^{-5}	2.25×10^{-4}	1.25×10^{-7}	2.26×10^{-7}
ν^c (GeV)	m_{h_1} (GeV)	m_{h_2} (GeV)	m_{h_3} (GeV)	m_{h_4} (GeV)	m_{P_1} (GeV)
8.0×10^2	19.8	21.6	21.8	120.2	8.8
m_{P_2} (GeV)	m_{P_3} (GeV)	$m_{\tilde{\chi}_4^0}$ (GeV)	$m_{\tilde{\chi}_5^0}$ (GeV)	$m_{\tilde{\chi}_6^0}$ (GeV)	—
8.9	16.9	26.3	26.5	27.8	—
$BR(h_4 \rightarrow h_1 h_1)$	$BR(h_4 \rightarrow P_3 P_3)$	$BR(h_4 \rightarrow \sum_{i,j=4}^6 \tilde{\chi}_i^0 \tilde{\chi}_j^0)$	$BR(h_4 \rightarrow b\bar{b})$	$BR(h_1 \rightarrow \sum_{i,j=1}^2 P_i P_j)$	$BR(h_{2,3} \rightarrow \sum_{i,j=1}^2 P_i P_j)$
0.05	0.12	0.06	0.55	0.98	1.0
$BR(P_{1,2} \rightarrow \tau^+ \tau^-)$	$BR(P_3 \rightarrow b\bar{b})$	$BR(\tilde{\chi}_4^0 \rightarrow \sum_{i=1}^3 h_i \nu)$	$BR(\tilde{\chi}_4^0 \rightarrow P_{1,2} \nu)$	$BR(\tilde{\chi}_4^0 \rightarrow P_3 \nu)$	$l_{\tilde{\chi}_4^0}$ (cm)
0.88	0.93	0.51	0.33	0.16	15

Table 8: Relevant input parameters, masses and branching ratios of benchmark point 8.

hand, the Higgs sector is extended due to the presence of left- and right-handed sneutrinos mixing with the MSSM Higgses. On the other hand the breaking of R-parity, could lead to signatures different from the usual missing energy.

First, we have analyzed the mixings in the Higgs sector of the $\mu\nu$ SSM. Assuming three families of right-handed neutrino superfields, one obtains eight CP-even and seven CP-odd Higgses in the model. Although the three left-handed sneutrinos are basically decoupled from the rest of the Higgses, the mixing between Higgs doublets and right-handed sneutrinos is not necessarily small. In this work we have deduced general conditions to suppress the latter. This can be useful to obtain very light singlets avoiding collider constraints, but also to have a doublet-like Higgs as the lightest one being as heavy as possible.

Then, we have provided an overview of new decays in the Higgs sector with respect to other SUSY models with extra singlets like the NMSSM. Due to the extended Higgs sector, Higgs-to-Higgs cascade decays could be more complicated, as shown in subsection 3.2. In addition, the breaking of R-parity gives rise to new decays. LEP constraints have also been discussed in the context of the $\mu\nu$ SSM. For this, we have computed the couplings of the Higgses with Z bosons and the sum rules.

Finally, in Section 4 we have concentrated on Higgs decays that are genuine of the $\mu\nu$ SSM, and could serve to distinguish it from other SUSY models. We have provided benchmark points that should pass current constraints and are interesting for LHC. In

Benchmark point	Cascade	$\sigma(gg \rightarrow h_4) \times BR_{\text{cascade}} \text{ (fb)}$
1	$h_4 \rightarrow \tilde{\chi}_4^0 \tilde{\chi}_4^0 \rightarrow 2P2\nu \rightarrow 2b2\bar{b}2\nu$	270
	$h_4 \rightarrow \tilde{\chi}_4^0 \tilde{\chi}_4^0 \rightarrow 2h2\nu \rightarrow 4P2\nu \rightarrow 4b4\bar{b}2\nu$	44
2	$h_4 \rightarrow \tilde{\chi}_4^0 \tilde{\chi}_4^0 \rightarrow 2P2\nu \rightarrow 2\tau^+ 2\tau^- 2\nu$	1620
3	$h_4 \rightarrow \tilde{\chi}_4^0 \tilde{\chi}_4^0 \rightarrow 2P2\nu \rightarrow 2b2\bar{b}2\nu$	70
4	$h_4 \rightarrow \tilde{\chi}_4^0 \tilde{\chi}_4^0 \rightarrow 2P2\nu \rightarrow 2b2\bar{b}2\nu$	5860
5	$h_4 \rightarrow \tilde{\chi}_4^0 \tilde{\chi}_4^0 \rightarrow 2P2\nu \rightarrow 2b2\bar{b}2\nu$	4870
6	$h_1 \rightarrow \tilde{\chi}_4^0 \tilde{\chi}_4^0 \rightarrow 2l2q2\bar{q}$	150
	$h_1 \rightarrow \tilde{\chi}_4^0 \tilde{\chi}_4^0 \rightarrow 2\nu 2l2\bar{l}$	80
	$h_1 \rightarrow \tilde{\chi}_4^0 \tilde{\chi}_4^0 \rightarrow 2\nu 2q2\bar{q}$	40
	$h_1 \rightarrow \tilde{\chi}_4^0 \tilde{\chi}_4^0 \rightarrow 6\nu$	15
7	$h_4 \rightarrow 2P \rightarrow 2b2\bar{b}$	5450
	$h_4 \rightarrow 2h_1 \rightarrow 4P \rightarrow 4b4\bar{b}$	460
8	$h_4 \rightarrow 2P_3 \rightarrow 2b2\bar{b}$	1660
	$h_4 \rightarrow h_1 h_1 \rightarrow 4P_{1,2} \rightarrow 4\tau^+ 4\tau^-$	460
	$h_4 \rightarrow \tilde{\chi}_4^0 \tilde{\chi}_4^0 \rightarrow 2P_{1,2} 2\nu \rightarrow 2\tau^+ 2\tau^- 2\nu$	80
	$h_4 \rightarrow \tilde{\chi}_4^0 \tilde{\chi}_4^0 \rightarrow 2h2\nu \rightarrow 4P_{1,2} 2\nu \rightarrow 4\tau^+ 4\tau^- 2\nu$	150
	$h_4 \rightarrow \tilde{\chi}_4^0 \tilde{\chi}_4^0 \rightarrow 2P_3 2\nu \rightarrow 2b2\bar{b}2\nu$	20

Table 9: Production cross section multiplied by branching ratios of the cascades, for the benchmark points discussed in the text.

particular, we have focused first our attention on the decays of a MSSM-like light Higgs h_{MSSM} with a sizeable branching ratio to two lightest neutralinos. These neutralinos could decay inside the detector leading to displaced vertices. This fact can be used to distinguish the $\mu\nu$ SSM from R -parity conserving models such as the NMSSM/MSSM. Let us remark, however, that in models of gauge mediated SUSY breaking, where the gravitino is the LSP, a displaced vertex can also be obtained depending on the lifetime of the next-to-LSP.

Besides, the decays can be into a neutrino and an on-shell light singlet pseudoscalar P , that subsequently decays into $b\bar{b}$ (or if kinematically forbidden into $\tau^+\tau^-$), and therefore the decay $h_{MSSM} \rightarrow \tilde{\chi}^0 \tilde{\chi}^0 \rightarrow 2P2\nu \rightarrow 2b2\bar{b}2\nu$ is genuine of the $\mu\nu$ SSM. For example, in other R -parity breaking models such as the BRpV, there are no singlet Higgses and a lightest neutralino lighter than gauge bosons could decay only through three-body decay processes. However, as the final products of the cascades can be the same in both models, it may be difficult to distinguish them experimentally. We have also seen that a final state with 8 b -jets plus missing energy is possible in situations where singlet-like scalars are produced first by the decay of the neutralino, and they decay into pseudoscalars, $h_{MSSM} \rightarrow \tilde{\chi}^0 \tilde{\chi}^0 \rightarrow 2h2\nu \rightarrow 4P2\nu \rightarrow 4b4\bar{b}2\nu$.

We have also studied a case with an spectrum similar to the one of the MSSM, where all CP-even singlet scalars are above 114 GeV , and the pseudoscalars are heavier than the neutralinos. Then, the h_{MSSM} will decay in a significant ratio to neutralinos, and these will decay only through three-body processes leading to displaced vertices.

In another case the neutralino does not play an important role and only Higg-to-Higgs

cascade decays are relevant. Although displaced vertices are not expected, the decays $h_{MSSM} \rightarrow 2P \rightarrow 2b2\bar{b}$, $h_{MSSM} \rightarrow 2h \rightarrow 4P \rightarrow 4b4\bar{b}$ are possible, allowing to distinguish the $\mu\nu$ SSM from other R-parity violating models. Besides, once a SUSY particle is produced at the collider, decaying into the LSP, the displaced vertex would allow to distinguish the $\mu\nu$ SSM from the NMSSM.

Finally, we have studied a case where for singlet-like pseudoscalars $P_{1,2}$ the decay into $b\bar{b}$ is kinematically forbidden, but for P_3 is allowed. Then, several interesting cascade decays are expected without leading to displaced vertices: $h_{MSSM} \rightarrow 2h_1 \rightarrow 4P_{1,2} \rightarrow 4\tau^+4\tau^-$, $h_{MSSM} \rightarrow 2P_3 \rightarrow 2b2\bar{b}$. This is a genuine feature of the $\mu\nu$ SSM. In addition, the following cascades are possible, with displaced vertices and missing energy: $h_{MSSM} \rightarrow \tilde{\chi}_4^0\tilde{\chi}_4^0 \rightarrow 2P_{1,2}2\nu \rightarrow 2\tau^+2\tau^-2\nu$, $h_{MSSM} \rightarrow \tilde{\chi}_4^0\tilde{\chi}_4^0 \rightarrow 2h_{1,2,3}2\nu \rightarrow 4P_{1,2}2\nu \rightarrow 4\tau^+4\tau^-2\nu$, $h_{MSSM} \rightarrow \tilde{\chi}_4^0\tilde{\chi}_4^0 \rightarrow 2P_32\nu \rightarrow 2b2\bar{b}2\nu$.

In conclusion, the above discussion gives us the idea that extremely characteristic cascades can be expected in certain regions of the parameter space of the $\mu\nu$ SSM.

We have also emphasized that in the $\mu\nu$ SSM the gravitino could be a viable dark matter candidate, accessible to indirect detection experiments, and without altering the collider phenomenology described along this paper. In particular, the branching ratio of neutralino to gravitino-photon turns out to be negligible.

Let us finally remark that the collider phenomenology of the $\mu\nu$ SSM is very rich and peculiar, as shown here using several benchmark points, and, as a consequence, we still need to carry out much work in the future to cover all interesting aspects of the model. For example, although we have discussed in Section 4 in some detail the detectability of the signals at the LHC, computing the production cross section multiplied by the branching ratios for the different cascades, the analysis with an event generator is beyond the scope of this paper and is left for a future work.

Acknowledgments

D.E. López-Fogliani would like to thank Ulrich Ellwanger for extremely helpful conversations. The work of J. Fidalgo and C. Muñoz was supported in part by MICINN under grants FPA2009-08958 and FPA2009-09017, by the Comunidad de Madrid under grant HEPHACOS S2009/ESP-1473, and by the European Union under the Marie Curie-ITN program PITN-GA-2009-237920. The work of D.E. López-Fogliani was supported by the French ANR TAPDMS ANR-09-JCJC-0146. The work of R. Ruiz de Austri was supported by MICINN under the project PARSIFAL FPA2007-60323. The authors also acknowledge the support of the Consolider-Ingenio 2010 Programme under grant MultiDark CSD2009-00064.

A. Neutral scalar mass matrices

A.1 CP-even neutral scalars

The quadratic potential includes

$$V_{\text{quadratic}} = \frac{1}{2} \mathbf{h}'_{\alpha} M_{h_{\alpha\beta}}^2 \mathbf{h}'_{\beta} + \dots, \quad (\text{A.1})$$

where $\mathbf{h}'_{\alpha} = (h_d, h_u, (\tilde{\nu}_i^c)^R, (\tilde{\nu}_i)^R)$ is in the unrotated basis, and below we give the expressions for the independent coefficients of $M_{h_{\alpha\beta}}^2$

$$M_{h_d h_d}^2 = m_{H_d}^2 + \frac{G^2}{4} \{3v_d^2 - v_u^2 + \nu_i \nu_i\} + \lambda_i \lambda_j \nu_i^c \nu_j^c + \lambda_i \lambda_i v_u^2, \quad (\text{A.2})$$

$$M_{h_u h_u}^2 = m_{H_u}^2 + \frac{G^2}{4} (-v_d^2 + 3v_u^2 - \nu_i \nu_i) + \lambda_i \lambda_j \nu_i^c \nu_j^c + \lambda_i \lambda_i v_d^2 \\ - 2Y_{\nu_{ij}} \lambda_j v_d \nu_i + Y_{\nu_{ik}} Y_{\nu_{ij}} \nu_j^c \nu_k^c + Y_{\nu_{ik}} Y_{\nu_{jk}} \nu_i \nu_j, \quad (\text{A.3})$$

$$M_{h_d h_u}^2 = -a_{\lambda_i} \nu_i^c - \frac{G^2}{2} v_d v_u + 2v_d v_u \lambda_i \lambda_i - (\lambda_k \kappa_{ijk} \nu_i^c \nu_j^c + 2Y_{\nu_{ij}} \lambda_j v_u \nu_i), \quad (\text{A.4})$$

$$M_{h_d (\tilde{\nu}_i^c)^R}^2 = -a_{\lambda_i} v_u + 2\lambda_i \lambda_j v_d \nu_j^c - 2\lambda_k \kappa_{ijk} v_u \nu_j^c - Y_{\nu_{ji}} \lambda_k \nu_j \nu_k^c - Y_{\nu_{jk}} \lambda_i \nu_j \nu_k^c, \quad (\text{A.5})$$

$$M_{h_u (\tilde{\nu}_i^c)^R}^2 = -a_{\lambda_i} v_d + a_{\nu_{ji}} \nu_j + 2\lambda_i \lambda_j v_u \nu_j^c - 2\lambda_k \kappa_{ilk} v_d \nu_l^c + 2Y_{\nu_{jk}} \kappa_{ilk} \nu_j \nu_l^c + 2Y_{\nu_{jk}} Y_{\nu_{ji}} v_u \nu_k^c, \quad (\text{A.6})$$

$$M_{h_d (\tilde{\nu}_i)^R}^2 = \frac{1}{2} G^2 v_d \nu_i - (Y_{\nu_{ij}} \lambda_j v_u^2 + Y_{\nu_{ij}} \lambda_k \nu_k^c \nu_j^c), \quad (\text{A.7})$$

$$M_{h_u (\tilde{\nu}_i)^R}^2 = a_{\nu_{ij}} \nu_j^c - \frac{G^2}{2} v_u \nu_i - 2Y_{\nu_{ij}} \lambda_j v_d v_u + Y_{\nu_{ik}} \kappa_{ljk} \nu_l^c \nu_j^c + 2Y_{\nu_{ij}} Y_{\nu_{kj}} v_u \nu_k, \quad (\text{A.8})$$

$$M_{(\tilde{\nu}_i)^R (\tilde{\nu}_j)^R}^2 = m_{\tilde{L}_{ij}}^2 + \frac{G^2}{2} \nu_i \nu_j + \frac{1}{4} G^2 (\nu_k \nu_k + v_d^2 - v_u^2) \delta_{ij} + Y_{\nu_{ik}} Y_{\nu_{jk}} v_u^2 + Y_{\nu_{ik}} Y_{\nu_{jl}} \nu_k^c \nu_l^c, \quad (\text{A.9})$$

$$M_{(\tilde{\nu}_i)^R (\tilde{\nu}_j^c)^R}^2 = a_{\nu_{ij}} v_u - Y_{\nu_{ij}} \lambda_k v_d \nu_k^c - Y_{\nu_{ik}} \lambda_j v_d \nu_k^c + 2Y_{\nu_{ik}} \kappa_{jlk} v_u \nu_l^c \\ + Y_{\nu_{ij}} Y_{\nu_{kl}} \nu_k \nu_l^c + Y_{\nu_{il}} Y_{\nu_{kj}} \nu_k \nu_l^c, \quad (\text{A.10})$$

$$M_{(\tilde{\nu}_i^c)^R (\tilde{\nu}_j^c)^R}^2 = m_{\tilde{\nu}_{ij}^c}^2 + 2a_{\kappa_{ijk}} \nu_k^c - 2\lambda_k \kappa_{ijk} v_d v_u + 2\kappa_{ijk} \kappa_{lmk} \nu_l^c \nu_m^c + 4\kappa_{ilk} \kappa_{jmk} \nu_l^c \nu_m^c \\ + \lambda_i \lambda_j (v_d^2 + v_u^2) + 2Y_{\nu_{lk}} \kappa_{ijk} v_u \nu_l - (Y_{\nu_{ki}} \lambda_i + Y_{\nu_{ki}} \lambda_j) v_d \nu_k + Y_{\nu_{ki}} Y_{\nu_{kj}} v_u^2 + Y_{\nu_{ki}} Y_{\nu_{jl}} \nu_k \nu_l. \quad (\text{A.11})$$

Then the mass eigenvectors are

$$\mathbf{h}_{\alpha} = R_{\alpha\beta}^h \mathbf{h}'_{\beta}, \quad (\text{A.12})$$

with the diagonal mass matrix

$$(M_{h_{\alpha\beta}}^{\text{diag}})^2 = R_{\alpha\gamma}^h M_{h_{\gamma\delta}}^2 R_{\beta\delta}^h. \quad (\text{A.13})$$

A.2 CP-odd neutral scalars

In the unrotated basis $\mathbf{P}'_\alpha = (P_d, P_u, (\tilde{\nu}_i^c)^I, (\tilde{\nu}_i)^I)$ we have

$$V_{\text{quadratic}} = \frac{1}{2} \mathbf{P}'_\alpha M_{P_{\alpha\beta}}^2 \mathbf{P}'_\beta + \dots \quad (\text{A.14})$$

Below we give the expressions for the independent coefficients of $M_{P_{\alpha\beta}}^2$

$$M_{P_d P_d}^2 = m_{H_d}^2 + \frac{G^2}{4} (v_d^2 - v_u^2 + \nu_i \nu_i) + \lambda_i \lambda_j \nu_i^c \nu_j^c + \lambda_i \lambda_i v_u^2, \quad (\text{A.15})$$

$$M_{P_u P_u}^2 = m_{H_u}^2 + \frac{G^2}{4} (v_u^2 - v_d^2 - \nu_i \nu_i) + \lambda_i \lambda_j \nu_i^c \nu_j^c + \lambda_i \lambda_i v_d^2 \\ - 2Y_{\nu_{ij}} \lambda_j v_d \nu_i + Y_{\nu_{ik}} Y_{\nu_{ij}} \nu_k^c \nu_j^c + Y_{\nu_{ik}} Y_{\nu_{jk}} \nu_i \nu_j, \quad (\text{A.16})$$

$$M_{P_d P_u}^2 = a_{\lambda_i} \nu_i^c + \lambda_k \kappa_{ijk} \nu_i^c \nu_j^c, \quad (\text{A.17})$$

$$M_{P_d (\tilde{\nu}_i^c)^I}^2 = a_{\lambda_i} v_u - 2\lambda_k \kappa_{ijk} v_u \nu_j^c - Y_{\nu_{ji}} \lambda_k \nu_k^c \nu_j + Y_{\nu_{jk}} \lambda_i \nu_k^c \nu_j, \quad (\text{A.18})$$

$$M_{P_d (\tilde{\nu}_i)^I}^2 = -Y_{\nu_{ij}} \lambda_j v_u^2 - Y_{\nu_{ij}} \lambda_k \nu_k^c \nu_j^c, \quad (\text{A.19})$$

$$M_{P_u (\tilde{\nu}_i^c)^I}^2 = a_{\lambda_i} v_d - a_{\nu_{ji}} \nu_j - 2\lambda_k \kappa_{ilk} v_d \nu_l^c + 2Y_{\nu_{jk}} \kappa_{ilk} \nu_j \nu_l^c, \quad (\text{A.20})$$

$$M_{P_u (\tilde{\nu}_i)^I}^2 = -a_{\nu_{ij}} \nu_j^c - Y_{\nu_{ik}} \kappa_{ljk} \nu_l^c \nu_j^c, \quad (\text{A.21})$$

$$M_{(\tilde{\nu}_i)^I (\tilde{\nu}_j)^I}^2 = m_{\tilde{L}_{ij}}^2 + \frac{1}{4} G^2 (\nu_k \nu_k + v_d^2 - v_u^2) \delta_{ij} + Y_{\nu_{ik}} Y_{\nu_{jk}} v_u^2 + Y_{\nu_{ik}} Y_{\nu_{jl}} \nu_k^c \nu_l^c, \quad (\text{A.22})$$

$$M_{(\tilde{\nu}_i)^I (\tilde{\nu}_j^c)^I}^2 = -a_{\nu_{ij}} v_u - Y_{\nu_{ik}} \lambda_j v_d \nu_k^c - Y_{\nu_{ij}} Y_{\nu_{lk}} \nu_l \nu_k^c + Y_{\nu_{ik}} Y_{\nu_{lj}} \nu_l \nu_k^c + Y_{\nu_{ij}} \lambda_k v_d \nu_k^c + 2Y_{\nu_{il}} \kappa_{jlk} v_u \nu_k^c, \quad (\text{A.23})$$

$$M_{(\tilde{\nu}_i^c)^I (\tilde{\nu}_j^c)^I}^2 = m_{\tilde{\nu}_{ij}^c}^2 - 2a_{\kappa_{ijk}} \nu_k^c + 2\lambda_k \kappa_{ijk} v_d v_u - 2\kappa_{ijk} \kappa_{lmk} \nu_l^c \nu_m^c + 4\kappa_{imk} \kappa_{ljk} \nu_l^c \nu_m^c \\ + \lambda_i \lambda_j (v_d^2 + v_u^2) - (Y_{\nu_{ki}} \lambda_j + Y_{\nu_{kj}} \lambda_i) v_d \nu_k - 2Y_{\nu_{lk}} \kappa_{ijk} v_u \nu_l + Y_{\nu_{ki}} Y_{\nu_{kj}} v_u^2 + Y_{\nu_{li}} Y_{\nu_{kj}} \nu_k \nu_l. \quad (\text{A.24})$$

Then the mass eigenvectors are

$$\mathbf{P}_\alpha = R_{\alpha\beta}^P \mathbf{P}'_\beta, \quad (\text{A.25})$$

with the diagonal mass matrix

$$(M_{P_{\alpha\beta}}^{\text{diag}})^2 = R_{\alpha\gamma}^P M_{P_{\gamma\delta}}^2 R_{\beta\delta}^P. \quad (\text{A.26})$$

B. Higgs sector couplings

B.1 Coupling between three CP-even Higgses

$h_\delta h_\epsilon h_\eta :$

$$\begin{aligned}
& \frac{\lambda_i \lambda_j}{\sqrt{2}} [\nu_i^c (\Pi_{\delta\epsilon\eta}^{11(j+2)} + \Pi_{\delta\epsilon\eta}^{22(j+2)}) + v_d \Pi_{\delta\epsilon\eta}^{1(i+2)(j+2)} + v_u \Pi_{\delta\epsilon\eta}^{2(i+2)(j+2)}] \\
& + \frac{1}{\sqrt{2}} \lambda_l \lambda_l [v_d \Pi_{\delta\epsilon\eta}^{122} + v_u \Pi_{\delta\epsilon\eta}^{211}] - \frac{1}{\sqrt{2}} \lambda_l \kappa_{ljk} [v_d \Pi_{\delta\epsilon\eta}^{2(j+2)(k+2)} + v_u \Pi_{\delta\epsilon\eta}^{1(j+2)(k+2)} + 2\nu_j^c \Pi_{\delta\epsilon\eta}^{12(k+2)}] \\
& + \sqrt{2} \kappa_{ljk} \kappa_{lbd} [\nu_j^c \Pi_{\delta\epsilon\eta}^{(k+2)(b+2)(d+2)}] + \frac{Y_{\nu_{ij}} Y_{\nu_{kl}}}{\sqrt{2}} [\nu_i \Pi_{\delta\epsilon\eta}^{(j+2)(l+2)(k+5)} + \nu_j^c \Pi_{\delta\epsilon\eta}^{(l+2)(i+5)(k+5)}] \\
& - \frac{1}{\sqrt{2}} Y_{\nu_{ij}} \lambda_k [\nu_i \Pi_{\delta\epsilon\eta}^{1(j+2)(k+2)} + \nu_j^c \Pi_{\delta\epsilon\eta}^{1(k+2)(i+5)} + \nu_k^c \Pi_{\delta\epsilon\eta}^{1(j+2)(i+5)} + v_d \Pi_{\delta\epsilon\eta}^{(j+2)(k+2)(i+5)}] \\
& + \frac{1}{\sqrt{2}} Y_{\nu_{ij}} Y_{\nu_{lm}} [v_u \Pi_{\delta\epsilon\eta}^{2(j+2)(m+2)} + \nu_j^c \Pi_{\delta\epsilon\eta}^{22(m+2)}] + \frac{1}{\sqrt{2}} Y_{\nu_{il}} Y_{\nu_{jl}} [v_u \Pi_{\delta\epsilon\eta}^{2(i+5)(j+5)} + \nu_i \Pi_{\delta\epsilon\eta}^{22(j+5)}] \\
& - \frac{1}{\sqrt{2}} \lambda_l Y_{\nu_{il}} [2v_u \Pi_{\delta\epsilon\eta}^{12(i+5)} + v_d \Pi_{\delta\epsilon\eta}^{22(i+5)} + \nu_i \Pi_{\delta\epsilon\eta}^{122}] \\
& + \frac{1}{\sqrt{2}} \kappa_{ljk} Y_{\nu_{il}} [2\nu_j^c \Pi_{\delta\epsilon\eta}^{2(k+2)(i+5)} + v_u \Pi_{\delta\epsilon\eta}^{(j+2)(k+2)(i+5)} + \nu_i \Pi_{\delta\epsilon\eta}^{2(j+2)(k+2)}] \\
& - \frac{1}{\sqrt{2}} (A_\lambda \lambda)_i \Pi_{\delta\epsilon\eta}^{12(i+2)} + \frac{1}{\sqrt{2}} (A_\nu Y_\nu)_{ij} \Pi_{\delta\epsilon\eta}^{2(i+2)(j+5)} + \frac{1}{3\sqrt{2}} (A_\kappa \kappa)_{ijk} \Pi_{\delta\epsilon\eta}^{(i+2)(j+2)(k+2)} \\
& + \frac{g_1^2 + g_2^2}{4\sqrt{2}} [\nu_i \Pi_{\delta\epsilon\eta}^{(i+5)(j+5)(j+5)} + \nu_i \Pi_{\delta\epsilon\eta}^{11(i+5)} - \nu_i \Pi_{\delta\epsilon\eta}^{22(i+5)} \\
& + v_d \Pi_{\delta\epsilon\eta}^{1(i+5)(i+5)} + v_d \Pi_{\delta\epsilon\eta}^{111} - v_d \Pi_{\delta\epsilon\eta}^{122} - v_u \Pi_{\delta\epsilon\eta}^{2(i+5)(i+5)} + v_u \Pi_{\delta\epsilon\eta}^{222} - v_u \Pi_{\delta\epsilon\eta}^{112}] , \tag{B.1}
\end{aligned}$$

where $b, d, i, j, k, l, m = 1, 2, 3$; $\alpha, \beta, \gamma, \delta, \epsilon, \eta = 1, \dots, 8$, and

$$\Pi_{\delta\epsilon\eta}^{\alpha\beta\gamma} = R_{\delta\alpha}^h R_{\epsilon\beta}^h R_{\eta\gamma}^h + R_{\delta\alpha}^h R_{\eta\beta}^h R_{\epsilon\gamma}^h + R_{\epsilon\alpha}^h R_{\delta\beta}^h R_{\eta\gamma}^h + R_{\epsilon\alpha}^h R_{\eta\beta}^h R_{\delta\gamma}^h + R_{\eta\alpha}^h R_{\delta\beta}^h R_{\epsilon\gamma}^h + R_{\eta\alpha}^h R_{\epsilon\beta}^h R_{\delta\gamma}^h . \tag{B.2}$$

B.2 Coupling between one CP-even and two CP-odd Higgses

$h_\delta P_\epsilon P_\eta :$

$$\begin{aligned}
& \frac{\lambda_i \lambda_j}{\sqrt{2}} [\nu_i^c (\Pi_{\delta\epsilon\eta}^{(j+2)11} + \Pi_{\delta\epsilon\eta}^{(j+2)22}) + v_d \Pi_{\delta\epsilon\eta}^{1(i+2)(j+2)} + v_u \Pi_{\delta\epsilon\eta}^{2(i+2)(j+2)}] + \frac{1}{\sqrt{2}} \lambda_l \lambda_l [v_d \Pi_{\delta\epsilon\eta}^{122} + v_u \Pi_{\delta\epsilon\eta}^{211}] \\
& + \frac{1}{\sqrt{2}} \lambda_l \kappa_{ljk} [v_d (\Pi_{\delta\epsilon\eta}^{2(j+2)(k+2)} - 2\Pi_{\delta\epsilon\eta}^{(j+2)2(k+2)}) + v_u (\Pi_{\delta\epsilon\eta}^{1(j+2)(k+2)} - 2\Pi_{\delta\epsilon\eta}^{(j+2)1(k+2)}) \\
& + 2\nu_j^c (\Pi_{\delta\epsilon\eta}^{(k+2)12} - \Pi_{\delta\epsilon\eta}^{12(k+2)} - \Pi_{\delta\epsilon\eta}^{21(k+2)})] \\
& + \sqrt{2} \kappa_{ljk} \kappa_{lbd} [-\nu_j^c \Pi_{\delta\epsilon\eta}^{(k+2)(b+2)(d+2)} + 2\nu_j^c \Pi_{\delta\epsilon\eta}^{(b+2)(k+2)(d+2)}] \\
& - \frac{\lambda_l Y_{\nu il}}{\sqrt{2}} [v_d \Pi_{\delta\epsilon\eta}^{(i+5)22} + \nu_i \Pi_{\delta\epsilon\eta}^{122} + 2v_u \Pi_{\delta\epsilon\eta}^{21(i+5)}] \\
& + \frac{\kappa_{ljk} Y_{\nu il}}{\sqrt{2}} [2\nu_j^c \Pi_{\delta\epsilon\eta}^{2(k+2)(i+5)} + 2\nu_j^c \Pi_{\delta\epsilon\eta}^{(i+5)2(k+2)} - 2\nu_j^c \Pi_{\delta\epsilon\eta}^{(k+2)2(i+5)} + 2v_u \Pi_{\delta\epsilon\eta}^{(j+2)(i+5)(k+2)} \\
& - v_u \Pi_{\delta\epsilon\eta}^{(i+5)(j+2)(k+2)} + 2\nu_i \Pi_{\delta\epsilon\eta}^{(j+2)2(k+2)} - \nu_i \Pi_{\delta\epsilon\eta}^{2(j+2)(k+2)}] \\
& - \frac{Y_{\nu ij} \lambda_k}{\sqrt{2}} [-\nu_i \Pi_{\delta\epsilon\eta}^{(j+2)(k+2)1} + \nu_i \Pi_{\delta\epsilon\eta}^{(k+2)(j+2)1} + \nu_i \Pi_{\delta\epsilon\eta}^{1(k+2)(j+2)} - \nu_j^c \Pi_{\delta\epsilon\eta}^{(i+5)(k+2)1} - \nu_j^c \Pi_{\delta\epsilon\eta}^{(k+2)(i+5)1} \\
& + \nu_j^c \Pi_{\delta\epsilon\eta}^{1(k+2)(i+5)} - \nu_k^c \Pi_{\delta\epsilon\eta}^{1(i+5)(j+2)} + \nu_k^c \Pi_{\delta\epsilon\eta}^{(i+5)1(j+2)} + \nu_k^c \Pi_{\delta\epsilon\eta}^{(j+2)1(i+5)} - v_d \Pi_{\delta\epsilon\eta}^{(k+2)(i+5)(j+2)} \\
& + v_d \Pi_{\delta\epsilon\eta}^{(j+2)(k+2)(i+5)} + v_d \Pi_{\delta\epsilon\eta}^{(i+5)(j+2)(k+2)}] + \frac{Y_{\nu ij} Y_{\nu kl}}{\sqrt{2}} [-\nu_i \Pi_{\delta\epsilon\eta}^{(j+2)(k+5)(l+2)} + \nu_i \Pi_{\delta\epsilon\eta}^{(l+2)(j+2)(k+5)} \\
& + \nu_i \Pi_{\delta\epsilon\eta}^{(k+5)(l+2)(j+2)} - \nu_j^c \Pi_{\delta\epsilon\eta}^{(i+5)(k+5)(l+2)} + \nu_j^c \Pi_{\delta\epsilon\eta}^{(k+5)(i+5)(l+2)} + \nu_j^c \Pi_{\delta\epsilon\eta}^{(l+2)(k+5)(i+5)}] \\
& + \frac{Y_{\nu ij} Y_{\nu lm}}{\sqrt{2}} [v_u \Pi_{\delta\epsilon\eta}^{2(j+2)(m+2)} + \nu_j^c \Pi_{\delta\epsilon\eta}^{(m+2)22}] + \frac{Y_{\nu il} Y_{\nu jl}}{\sqrt{2}} [v_u \Pi_{\delta\epsilon\eta}^{2(i+5)(j+5)} + \nu_i \Pi_{\delta\epsilon\eta}^{(j+5)22}] \\
& + \frac{(A_\lambda \lambda)_i}{\sqrt{2}} [\Pi_{\delta\epsilon\eta}^{(12(i+2))} + \Pi_{\delta\epsilon\eta}^{21(i+2)} + \Pi_{\delta\epsilon\eta}^{(i+2)12}] - \frac{(A_\nu Y_\nu)_{ij}}{\sqrt{2}} [\Pi_{\delta\epsilon\eta}^{2(i+5)(j+2)} + \Pi_{\delta\epsilon\eta}^{(i+5)2(j+2)} \\
& + \Pi_{\delta\epsilon\eta}^{(i+2)2(j+5)}] - \frac{(A_\kappa \kappa)_{ijk}}{\sqrt{2}} \Pi_{\delta\epsilon\eta}^{(i+2)(j+2)(k+2)} + \frac{g_1^2 + g_2^2}{4\sqrt{2}} [\nu_i \Pi_{\delta\epsilon\eta}^{(i+5)(j+5)(j+5)} + \nu_i \Pi_{\delta\epsilon\eta}^{(i+5)11} \\
& - \nu_i \Pi_{\delta\epsilon\eta}^{(i+5)22} + v_d (\Pi_{\delta\epsilon\eta}^{1(i+5)(i+5)} + \Pi_{\delta\epsilon\eta}^{111} - \Pi_{\delta\epsilon\eta}^{122}) + v_u (\Pi_{\delta\epsilon\eta}^{222} - \Pi_{\delta\epsilon\eta}^{211} - \Pi_{\delta\epsilon\eta}^{2(i+5)(i+5)})] , \tag{B.3}
\end{aligned}$$

where $b, d, i, j, k, l, m = 1, 2, 3$; $\alpha, \beta, \gamma, \delta = 1, \dots, 8$; $\epsilon, \eta = 1, \dots, 7$, and

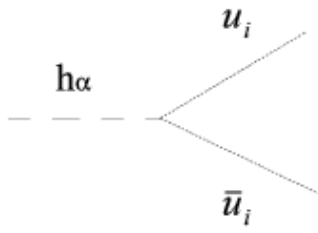
$$\Pi_{\delta\epsilon\eta}^{\alpha\beta\gamma} = R_{\delta\alpha}^h (R_{\epsilon\beta}^P R_{\eta\gamma}^P + R_{\eta\beta}^P R_{\epsilon\gamma}^P) . \tag{B.4}$$

References

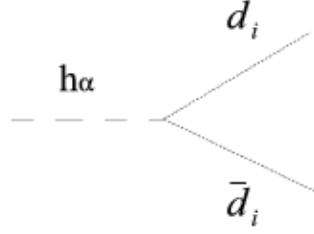
- [1] D. E. López-Fogliani and C. Muñoz, *Phys. Rev. Lett.* **97** (2006) 041801 [arXiv:hep-ph/0508297].
- [2] C. Muñoz, unpublished notes (1994).
- [3] For brief reviews, see: C. Muñoz, *AIP Conf. Proc.* **1200** (2010) 413 [arXiv:0909.5140 [hep-ph]]; D. E. López-Fogliani, arXiv:1004.0884 [hep-ph].
- [4] J. E. Kim and H. P. Nilles, *Phys. Lett.* **B138** (1984) 150.
- [5] For a review, see: S.P. Martin, in the book ‘Perspectives on supersymmetry II’, Ed. G.L. Kane, *World Scientific* (2010) 1 [arXiv:hep-ph/9709356].

- [6] For a review, see: U. Ellwanger, C. Hugonie and A.M. Teixeira, *Phys. Rept.* **496** (2010) 1 [arXiv:0910.1785 [hep-ph]].
- [7] N. Escudero, D. E. López-Fogliani, C. Muñoz and R. R. de Austri, *JHEP* **12** (2008) 099 [arXiv:0810.1507 [hep-ph]].
- [8] J. Fidalgo, D. E. Lopez-Fogliani, C. Munoz and R. Ruiz de Austri, *JHEP* **08** (2009) 105 [arXiv:0904.3112 [hep-ph]].
- [9] P. Ghosh and S. Roy, *JHEP* **04** (2009) 069 [arXiv:0812.0084 [hep-ph]].
- [10] P. Ghosh, P. Dey, B. Mukhopadhyaya and S. Roy, *JHEP* **05** (2010) 087 [arXiv:1002.2705 [hep-ph]].
- [11] For a review, see e.g.: C. Muñoz, *Int. J. Mod. Phys. A* **19** (2004) 3093 [arXiv:hep-ph/0309346].
- [12] See e.g.: D.G. Cerdeño, C. Muñoz and O. Seto, *Phys. Rev. D* **79** (2009) 023510 [arXiv:0807.3029 [hep-ph]], and references therein.
- [13] K. Y. Choi, D. E. López-Fogliani, C. Munoz and R. Ruiz de Austri, *JCAP* **03** (2010) 028 [arXiv:0906.3681[hep-ph]].
- [14] D. J.H. Chung and A. J. Long, *Phys. Rev. D* **81** (2010) 123531 [arXiv:1004.0942 [hep-ph]].
- [15] A. Bartl, M. Hirsch, A. Vicente, S. Liebler and W. Porod, *JHEP* **05** (2009) 120 [arXiv:0903.3596 [hep-ph]].
- [16] S. Liebler and W. Porod, arXiv:1106.2921 [hep-ph].
- [17] P. Bandyopadhyay, P. Ghosh and S. Roy, arXiv:1012.5762 [hep-ph].
- [18] U. Ellwanger and C. Hugonie, *Mod. Phys. Lett. A* **22** (2007) 1581 [arXiv:hep-ph/0612133].
- [19] LEP Higgs Working Group, LHWG Note/2002-02.
- [20] For a review, see: M. Hirsch and J.W.F. Valle, *New J. Phys.* **6** (2004) 76 [arXiv:hep-ph/0405015].
- [21] G. Abbiendi *et al.*, LEP Working Group for Higgs Boson Searches, *Phys. Lett. B* **565** (2003) 61 [arXiv:hep-ex/0306033].
- [22] G. Abbiendi *et al.* [OPAL Collaboration], *Eur. Phys. J. C* **37** (2004) 49 [arXiv:hep-ex/0406057].
- [23] G. Abdallah *et al.* [DELPHI Collaboration], *Eur. Phys. J. C* **38** (2004) 1 [arXiv:hep-ex/0410017].
- [24] R. Dermisek and J. F. Gunion, *Phys. Rev. D* **73** (2006) 111701 [hep-ph/0510322], *Phys. Rev. Lett.* **95** (2005) 041801 [hep-ph/0502105].
- [25] G. Abbiendi *et al.* [OPAL Collaboration], *Eur. Phys. J. C* **27** (2003) 311 [arXiv:hep-ex/0206022];
- [26] G. Abbiendi *et al.* [OPAL Collaboration], *Eur. Phys. J. C* **27** (2003) 483 [arXiv:hep-ex/0209068].
- [27] S. Schael *et al.* [ALEPH Collaboration], *JHEP* **05** (2010) 049 [arXiv:1003.0705 [hep-ex]].

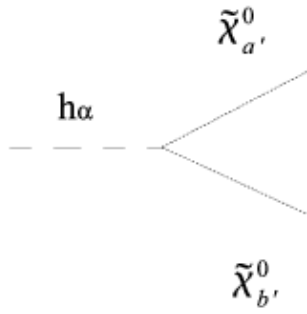
- [28] K. Hagiwara *et al.*, *Phys. Rev.* **D66** (2002) 010001; J. Abdallah *et al.* [DELPHI Collaboration], *Eur. Phys. J.* **C31** (2004) 421 [arXiv:hep-ex/0311019]; G. Abbiendi *et al.* [OPAL Collaboration], *Eur. Phys. J.* **C35** (2004) 1 [arXiv:hep-ex/0401026].
- [29] C. Panagiotakopoulos and A. Pilaftsis, *Phys. Rev.* **D63** (2001) 055003 [arXiv:hep-ph/0008268].
- [30] S. W. Ham, H. Genten, B. R. Kim and S. K. Oh, *Phys. Lett.* **B383** (1996) 179 [arXiv:hep-ph/9606361].
- [31] U. Ellwanger and C. Hugonie, *Comput. Phys. Commun.* **175** (2006) 290 [arXiv:hep-ph/0508022].
- [32] W. Porod, *Comput. Phys. Commun.* **153** (2003) 275 [arXiv:hep-ph/0301101].
- [33] G. L. Fogli *et al.*, *Phys. Rev.* **D78** (2008) 033010 [arXiv:0805.2517 [hep-ph]]; T. Schwetz, M. Tortola and J. W. F. Valle, *New J. Phys.* **13** (2011) 063004 [arXiv:1103.0734 [hep-ph]].
- [34] J. Abdallah *et al.*, LEP SUSY Working Group, <http://lepsusy.web.cern.ch/lepsusy/>
- [35] K. Nakamura *et al.* [Particle Data Group], *J. Phys.* **G37** (2010) 075021.
- [36] D. Buskulic *et al.* [ALEPH Collaboration], *Phys. Lett.* **B313** (1993) 312.
- [37] LEP Higgs Working Group, LHWG Note 2001-06, arXiv:hep-ex/0107032.
- [38] G. Abbiendi *et al.* [OPAL Collaboration], *Phys. Lett.* **B597** (2004) 11 [arXiv:hep-ex/0312042].
- [39] LEP Higgs Working Group, LHWG Note 2001-07, arXiv:hep-ex/0107034.
- [40] A. Belyaev, J. Pivarski, A. Safonov, S. Senkin and A. Tatarinov, *Phys. Rev.* **D81** (2010) 075021 [arXiv:1002.1956 [hep-ph]].
- [41] M. Spira, arXiv:hep-ph/9510347.
- [42] W. B. Atwood *et al.* [Fermi/LAT Collaboration], *Astrophys J.* **697** (2009) 1071 [arXiv:0902.1089 [astro-ph.IM]].
- [43] See e.g.: W. Buchmuller, L. Covi, K. Hamaguchi, A. Ibarra and T. Yanagida, *JHEP* **03** (2007) 037 [arXiv:hep-ph/0702184], and references therein.



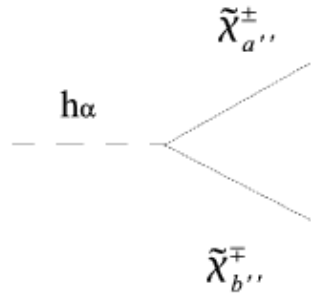
(a)



(b)



(c)



(d)

Figure 1: Feynman diagrams of Higgs decay to fermions, with $\alpha = 1, \dots, 8$, $i = 1, 2, 3$, $a', b' = 1, \dots, 10$, and $a'', b'' = 1, \dots, 5$. Replacing the decaying h_α by a pseudoscalar $P_{\alpha'}$, with $\alpha' = 1, \dots, 7$, all the Feynman diagrams are valid.

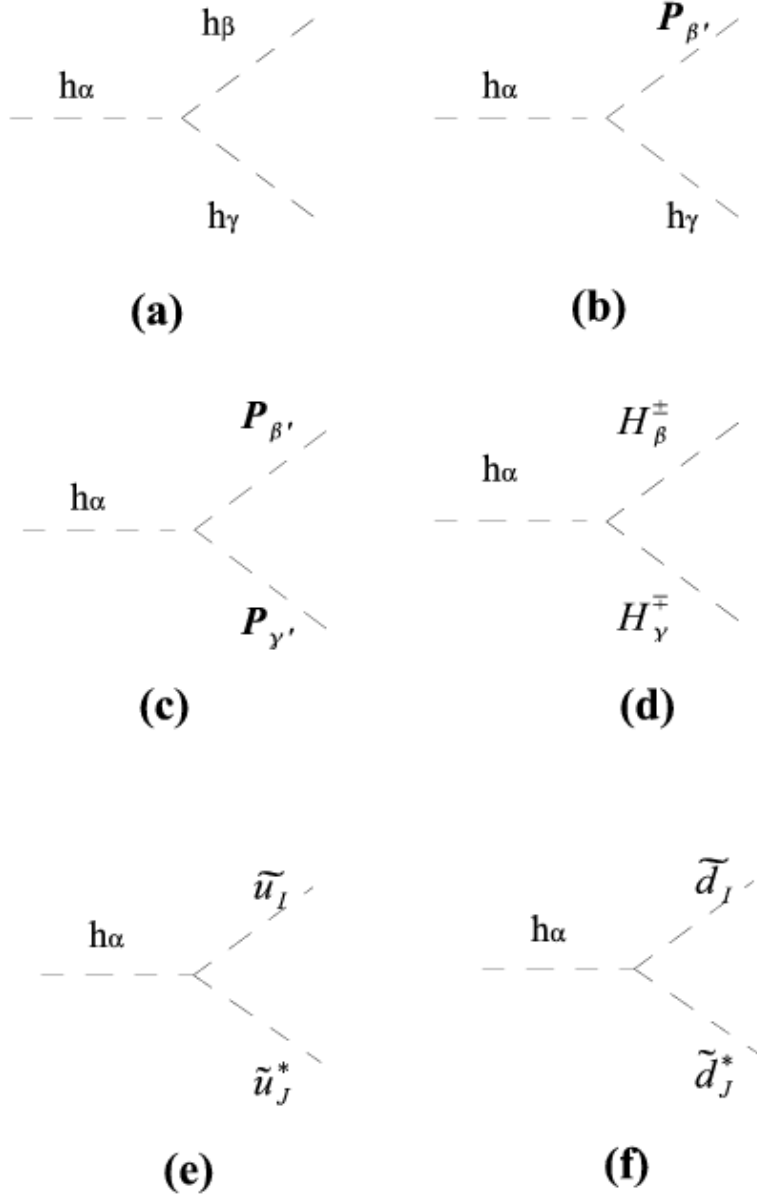


Figure 2: Feynman diagrams of Higgs decays to scalars (under Lorentz), with $I, J = 1..6$. Replacing the decaying h_α by a pseudoscalar $P_{\alpha'}$, all the Feynman diagrams are valid. The index convention is like in Fig. 1.

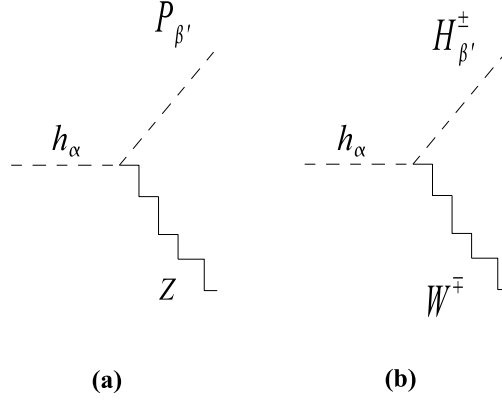


Figure 3: Feynman diagrams of Higgs decays to scalars and vectors (under Lorentz). Replacing the decaying h_α by a pseudoscalar $P_{\alpha'}$, all the Feynman diagrams are valid. The index convention is like in Fig. 1.

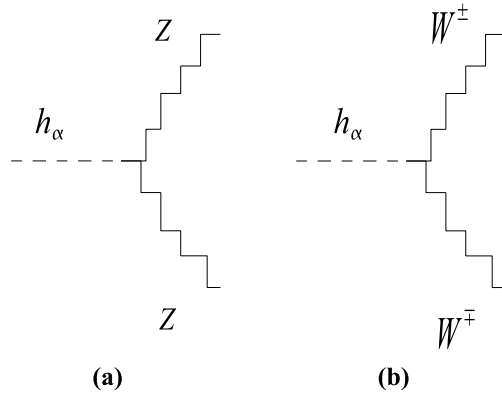


Figure 4: Feynman diagrams of Higgs decays to vectors (under Lorentz). The index convention is like in Fig. 1.

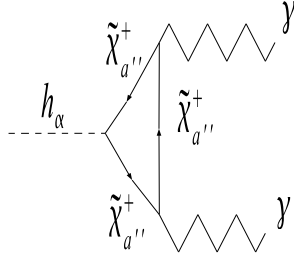


Figure 5: Di-photon Higgs decay. Replacing the decaying h_α by a pseudoscalar $P_{\alpha'}$, the Feynman diagram is valid. The index convention is like in Fig. 1.

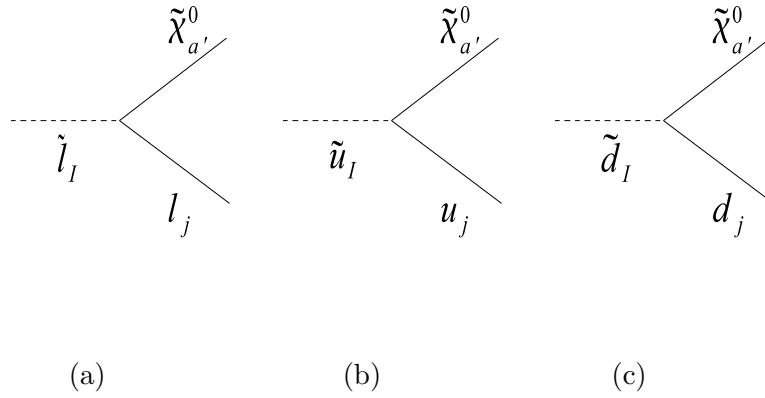


Figure 6: (a) Charged slepton decay. (b) Up squark decay. (c) Down squark decay. The index convention is like in Figs. 1 and 2.

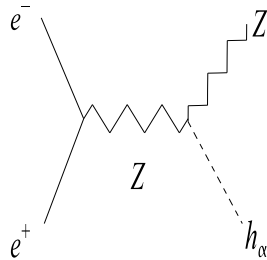


Figure 7: Higgs-strahlung. The index convention is like in Fig. 1.

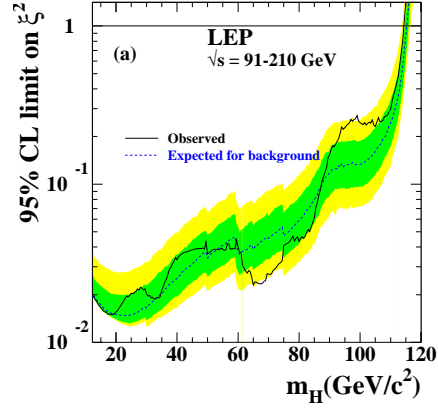


Figure 8: The 95% confidence level upper bound on the ratio $\xi^2 = (g_{hZZ}/g_{hZZ}^{SM})^2$ from [21]. The dark and light shaded bands around the median expected line correspond to the 68% and 95% probability bands. The horizontal line corresponds to the Standard Model coupling for Higgs boson decays predicted by the Standard Model.